


# *IncMGPF* is a novel positive regulator of muscle growth and regeneration

Wei Lv<sup>1</sup>, Jianjun Jin<sup>1</sup>, Zaiyan Xu<sup>1,3</sup>, Hongmei Luo<sup>1</sup>, Yubo Guo<sup>1</sup>, Xiaojing Wang<sup>1</sup>, Shanshan Wang<sup>1</sup>, Jiali Zhang<sup>1</sup>, Hao Zuo<sup>1</sup>, Wei Bai<sup>1</sup>, Yaxing Peng<sup>1</sup>, Junming Tang<sup>4</sup>, Shuhong Zhao<sup>1,2</sup> & Bo Zuo<sup>1,2\*</sup> 

<sup>1</sup>Key Laboratory of Swine Genetics and Breeding of Ministry of Agriculture and Rural Affairs & Key Laboratory of Agriculture Animal Genetics, Breeding and Reproduction of Ministry of Education, College of Animal Science and Technology, Huazhong Agricultural University, Wuhan, China, <sup>2</sup>The Cooperative Innovation Center for Sustainable Pig Production, Wuhan, China, <sup>3</sup>Department of Basic Veterinary Medicine, College of Veterinary Medicine, Huazhong Agricultural University, Wuhan, China, <sup>4</sup>Hubei Key Laboratory of Embryonic Stem Cell Research, School of Basic Medicine Science, Hubei University of Medicine, Shiyan, China

## Abstract

**Background** Long non-coding RNAs (lncRNAs) play critical regulatory roles in diverse biological processes and diseases. While a large number of lncRNAs have been identified in skeletal muscles until now, their function and underlying mechanisms in skeletal myogenesis remain largely unclear.

**Methods** We characterized a novel functional lncRNA designated *IncMGPF* (lncRNA muscle growth promoting factor) using RACE, Northern blot, fluorescence *in situ* hybridization and quantitative real-time PCR. Its function was determined by gene overexpression, interference, and knockout experiments in C2C12 myoblasts, myogenic progenitor cells, and an animal model. The molecular mechanism by which *IncMGPF* regulates muscle differentiation was mainly examined by cotransfection experiments, luciferase reporter assay, RNA immunoprecipitation, RNA pull-down, and RNA stability analyses.

**Results** We report that *IncMGPF*, which is highly expressed in muscles and positively regulated by myoblast determination factor (MyoD), promotes myogenic differentiation of muscle cells *in vivo* and *in vitro*. *IncMGPF* knockout in mice substantially decreases growth rate, reduces muscle mass, and impairs muscle regeneration. Overexpression of *IncMGPF* in muscles can rescue the muscle phenotype of knockout mice and promote muscle growth of wild-type mice. Mechanistically, *IncMGPF* promotes muscle differentiation by acting as a molecular sponge of miR-135a-5p and thus increasing the expression of myocyte enhancer factor 2C (*MEF2C*), as well as by enhancing human antigen R-mediated messenger RNA stabilization of myogenic regulatory genes such as *MyoD* and *myogenin* (*MyoG*). We confirm that pig lncRNA *AK394747* and human lncRNA *MT510647* are homologous to mouse *IncMGPF*, with conserved function and mechanism during myogenesis.

**Conclusions** Our data reveal that *IncMGPF* is a novel positive regulator of myogenic differentiation, muscle growth and regeneration in mice, pigs, and humans.

**Keywords** lncRNA; *IncMGPF*; Myogenesis; HuR; miR-135a-5p

Received: 16 November 2019; Revised: 24 July 2020; Accepted: 23 August 2020

\*Correspondence to: Bo Zuo, Key Laboratory of Swine Genetics and Breeding of Ministry of Agriculture and Rural Affairs & Key Laboratory of Agriculture Animal Genetics, Breeding and Reproduction of Ministry of Education, College of Animal Science and Technology, Huazhong Agricultural University, Wuhan, China.

Email: zuobo@mail.hzau.edu.cn

Wei Lv and Jianjun Jin contributed equally to the work.

## Introduction

Skeletal muscle plays important roles in activities of daily life and health. Abnormal regulation of skeletal muscle-specific genes leads to various muscle diseases, such as sarcopenia, myosarcoma, and muscle metabolic disorder.<sup>1,2</sup> Skeletal

muscle is the main agricultural animal protein source consumed by humans, and the growth and development of skeletal muscle directly impact the quantity and quality of meat.<sup>3</sup> Skeletal myogenesis is a process in which mesenchymal stem cells differentiate into myoblasts, which then proliferate, exit

the cell cycle, and fuse together to form mature myofibres, which determine the protein characteristics of muscle tissue.<sup>4</sup> When skeletal muscles are damaged postnatally, the muscle repair and regeneration processes parallel developmental myogenesis, with satellite cells located in niches on the myofibre surface being responsible for the generation of myoblasts.<sup>5</sup> The determination and terminal differentiation of muscle cells are primarily controlled by four myogenic regulatory factors (MRFs): myogenic factor 5, muscle-specific regulatory factor 4, myoblast determination factor (MyoD), and myogenin (MyoG).<sup>6</sup> MRFs activate numerous downstream genes to initiate muscle cell differentiation by cooperating with other transcription factors, such as myocyte enhancer factor 2 (MEF2), and in concert with epigenetic regulatory mechanisms.<sup>7,8</sup> In-depth exploration of MRF-mediated regulatory networks could contribute greatly to identifying molecular targets for treating muscle diseases and improving meat production.

In recent years, a large number of non-coding RNAs (ncRNAs) have been discovered and shown to be involved in the regulation of biological processes in almost all species. Among the ncRNAs, long non-coding RNAs (lncRNAs) are a class of RNA transcripts greater than 200 nt in length with little or no protein-coding capacity.<sup>9,10</sup> Substantial evidence has shown that lncRNAs play critical regulatory roles in diverse biological processes and diseases, such as X-chromosome inactivation,<sup>11</sup> genome imprinting,<sup>12</sup> stem cell pluripotency,<sup>13</sup> organ development,<sup>14</sup> immune responses,<sup>15</sup> drug resistance,<sup>16</sup> and tumorigenesis.<sup>17</sup> These lncRNAs function through multiple regulatory mechanisms, including chromatin modification, transcription activation, microRNA (miRNA) sponging, and mRNA splicing and translation.<sup>18</sup> In terms of myogenesis, tens of thousands of lncRNAs have been discovered in skeletal muscles using high-throughput technologies and bioinformatics analyses, but only a few of them have been identified as functional regulators of skeletal muscle development and regeneration; these include *H19*,<sup>19</sup> *SYSL*,<sup>20</sup> *linc-RAM*,<sup>21</sup> *Linc-MD1*,<sup>22</sup> *Inc-mg*,<sup>23</sup> *m1/2sbsRNAs*,<sup>24</sup> *Dum*,<sup>25</sup> *LncMyoD*,<sup>26</sup> *MAR1*,<sup>27</sup> and *LncIRS1*.<sup>28</sup> Therefore, the identification of novel functional lncRNAs involved in myogenesis, and elucidation of their mechanisms of action, requires more work.

In this study, we identified the muscle-enriched and MyoD-activated lncRNA *AK003290* in mice and its homologous lncRNA *AK394747* in pigs and *MT510647* in humans. Functional analyses revealed that *AK003290*, *AK394747*, and *MT510647* significantly promote myogenic differentiation and muscle growth; therefore, we named them *IncMGPF* (lncRNA muscle growth promoting factor). *IncMGPF* acts as a molecular sponge of miR-135a-5p, thus promoting MEF2C gene expression, and also regulates human antigen R (HuR; also known as ELAV-like RNA binding protein 1)-mediated mRNA stabilization of *MyoD* and *MyoG* genes. Our observations show that *IncMGPF* is a conserved positive regulator of skeletal muscle growth in mice, pigs, and humans.

## Materials and methods

### Animals

All procedures involving animals were performed in accordance with the guidelines of good laboratory practice, and animals were supplied with nutritious food and sufficient water. Animal feeding and tests were conducted based on the National Research Council Guide for the Care and Use of Laboratory Animals and approved by the Institutional Animal Care and Use Committee at Huazhong Agricultural University. Piglets were slaughtered according to a standard procedure based on guidelines in the Regulation of the Standing Committee of Hubei People's Congress (Hubei Province, China, HZAUSW-2017-008). All mice were obtained from the experimental animal centre of Huazhong Agricultural University. All pigs were obtained from the experimental pig farm of Huazhong Agricultural University.

### Primary myogenic progenitor cells isolation and cell culture

Mouse primary myogenic progenitor cells were isolated from 5-week-old C57BL mice; pig primary myogenic progenitor cells were isolated from 1-day-old large white male piglets. Primary myogenic progenitor cells were isolated and cultured as described previously.<sup>27,29</sup> Briefly, muscles were minced and digested in 2 mg/mL type I collagenase (C0130; Sigma-Aldrich, St. Louis, MO, USA). Digestion was stopped with RPMI 1640 medium containing 20% foetal bovine serum (FBS). Cells were cultured in growth medium [RPMI 1640 supplemented with 20% FBS, 4 ng/mL basic fibroblast growth factor, 1% chicken embryo extract, and 1% penicillin–streptomycin] on collagen-coated cell culture plates at 37°C and 5% CO<sub>2</sub>. C2C12 myoblasts, pig kidney (PK) cells, 293T cells, and HeLa cells were obtained from the Chinese Academy of Sciences Cell Bank and grown in incubators at 37°C and 5% CO<sub>2</sub>, and proliferating cells were cultured in Dulbecco's Modified Eagle's Medium (DMEM) supplemented with 10% FBS (Gibco, Grand Island, NY, USA). Human skeletal muscle myoblasts (Cat. #3501) were obtained from ScienCell Research Laboratories and grown in incubators at 37°C and 5% CO<sub>2</sub>, and proliferating cells were cultured in DMEM supplemented with 5% FBS (Gibco, Grand Island, NY, USA). For myogenic differentiation, cells were cultured in DMEM containing 2% horse serum (Gibco). All cells were grown to 80–90% confluence before differentiation was induced.

### Single myofibre isolation and culture

Single myofibres were isolated from extensor digitorum longus (EDL) muscles of mice, as described previously.<sup>30</sup>

Briefly, EDL muscles were separated and digested with 2 mg/mL collagenase I (C0130) in DMEM for 1 h at 37°C. Digestion was stopped by carefully transferring EDL muscles to a pre-warmed Petri dish (10 cm) with 6 mL of DMEM supplemented with 10% horse serum; the muscles were then lightly flushed with a P200 micropipette to release single myofibres. The released single myofibres were transferred and cultured in a Matrigel-coated Petri dish (10 cm) in DMEM supplemented with 20% FBS, 4 ng/mL basic fibroblast growth factor, and 1% penicillin–streptomycin at 37°C and 5% CO<sub>2</sub>.

### Total RNA extraction, microarray hybridization, and data analyses

Total RNA was isolated using TRIzol reagent (Invitrogen, USA) according to the manufacturer's instructions. The Mouse 4 × 44 K Gene Expression Microarray containing 34,456 probes was used to identify differentially expressed genes in C2C12 myoblasts that had differentiated for 2 days after knockdown of *lncMGPF* as described below. Six microarrays were used in the experiment, with three biological replicates of each treatment. Microarray hybridization was conducted according to the Expression Analysis Technical Manual (KangChen Bio-technology, China). Microarray data were analysed according to a previously reported method.<sup>20</sup> Differentially expressed mRNAs with statistically significant changes were identified through fold-change filtering ( $\geq 1.5$ ), unpaired *t*-tests ( $P < 0.05$ ), and multiple hypothesis testing (false discovery rate  $< 0.05$ ). Pathway analyses were based on Kyoto Encyclopedia of Genes and Genomes, and *P* values were used to determine the significance of the pathways (threshold  $P < 0.05$ ).

### Quantitative real-time PCR

Total RNA was reverse-transcribed using RevertAid Reverse Transcriptase (Thermo Scientific, USA). All miRNAs were reverse-transcribed using specific loop primer. Quantitative real-time PCR (qRT-PCR) analyses was performed using the Applied Biosystems StepOnePlus real-time PCR system. Relative RNA expression was calculated using the Ct ( $2^{-\Delta\Delta Ct}$ ) method.<sup>31</sup> All primers used in qRT-PCR are presented in Supporting Information, Table S1.

### Rapid amplification of complementary DNA ends

We performed 5' and 3' rapid amplification of complementary DNA ends (RACE) using the Takara SMARTer RACE complementary DNA amplification Kit (Clontech, USA) according to the manufacturer's instructions. The sequences of gene-specific primers used for *lncMGPF* RACE were 5'-CCTG

GGCTTCATTTACTCCTGAAGACAGTC-3' (5' RACE) and 5'-GCAGCCATCTTGGTGGAGAAGTTCCTGGC-3' (3' RACE). The sequences of gene-specific primers used for *AK394747* RACE were 5'-CCTGCCTCAAACCCCTCTTTACTCATCA-3' (5' RACE) and 5'-ATTGCCAGCATTTGTAAGTGATTGTGCAAT-3' (3' RACE). For the *lncMGPF* RACE assay, homologous sequences in the human genome were retrieved from NCBI database using Basic Local Alignment Search Tool, and confirmed by RT-PCR using forward (5'-ACAGTTTACAAGGTGTAGGT-3') and reverse (5'-TGAAAATGTGATTCTCAGAG-3') primers and sequencing. From the sequencing results, 5' and 3' RACE primers were designed. The sequences of gene-specific primers were 5'-GGGGTGCAAACCTACACCTTGTAAGT-3' (5' RACE) and 5'-GCAAAAAGTCCTTCCAGGGCTCCC-3' (3' RACE).

### Northern blot

Northern blot was performed according to a published method.<sup>32</sup> Total RNA from differentiated C2C12 myoblasts was extracted using a total RNA kit (Omega bio-tek, Norcross, GA, USA). Then, transferred the RNA to a positively charged nylon membrane and UV cross-linked, the p32-labelled probe was hybridized to the membrane at 60°C overnight. The *lncMGPF* RNA probe sequence was as follows: 5'-GCAGCCATCTTGGTGGAGAAGTTCCTGGC-3'.

### Nuclear and cytoplasmic RNA and protein fractionation

Nuclear and cytoplasmic RNA fractionation was performed according to a previously published method,<sup>21</sup> and distribution quantification was analysed via qRT-PCR. Nuclear and cytoplasmic protein fractionation was performed using the Nuclear and Cytoplasmic Protein Extraction Kit (Beyotime Biotechnology, China) according to the manufacturer's instructions, and the distribution was quantified using Western blotting.

### RNA fluorescence in situ hybridization

RNA fluorescence *in situ* hybridization (FISH) was performed using the lncRNA FISH Kit (Guangzhou RiboBio, China) according to the manufacturer's instructions. Briefly, cells were fixed with 4% formaldehyde for 10 min at room temperature. After washing, cells were permeabilized with 0.5% Triton X-100 for 30 min at 37°C. Then, cells were incubated with RNA probes in hybridization buffer overnight at 37°C. The RNA probes were directly conjugated with a fluorophore. Then, the cells were washed three times using saline sodium citrate buffer, stained with 4',6'-diamidino-2-phenylindole

(DAPI) for 10 min at room temperature, and examined using a fluorescence microscope.

### Luciferase reporter assay

*IncMGPF* promoter regions were cloned into a PGL3-basic luciferase reporter vector (Addgene, USA), and the constructed luciferase reporter vectors were transfected into C2C12 myoblasts in a 24-well plate. The 3' untranslated region (UTR) of *MEF2C*, sequences containing the miR-135a-5p binding site of *IncMGPF* or *AK394747*, and the sequences of *IncMGPF* or *AK394747* with mutated miR-135a-5p binding sites, were cloned into the pmirGLO Dual-Luciferase miRNA Target Expression Vector (Promega, USA) to construct the corresponding reporter vectors. Those reporter vectors were transfected into C2C12 myoblasts, HeLa cells, PK cells, and myogenic progenitor cells using Lipofectamine 2000. The luciferase assay was performed using the Dual-Luciferase Reporter Assay System (Promega, USA) and the enzymatic activity of luciferase measured using a PerkinElmer 2030 Multilabel Reader (PerkinElmer, USA).

### Small interfering RNA and microRNA synthesis and cell transfection

Small interfering RNAs (siRNAs) targeting *IncMGPF*, *AK394747*, *HuR*, and *MyoD*, as well as the inhibitor and mimics of miR-135a-5p, were synthesized by Genepharma (Genepharma, China); all siRNA sequences are presented in Supporting Information, Table S2. For cell transfection, we transfected C2C12 myoblasts, PK cells, HeLa cells, and mouse and pig myogenic progenitor cells with approximately 160  $\mu$ M siRNA oligonucleotides using 9  $\mu$ L Lipofectamine 2000 (Invitrogen, USA) in each well of a 6-well plate.

### Plasmid construction and transfection

To construct the *IncMGPF*, *MyoD*, *MEF2C*, *HuR*, and *AK394747* overexpression plasmids, the full-length or coding sequence of *IncMGPF*, *MyoD*, and *MEF2C* were cloned into the pcDNA3.1 plasmid (Addgene, USA). For *in vitro* translation assays, the coding sequence of *HuR* and predicted open reading frame sequence were cloned into the pCMV-C-enhanced green fluorescent protein (EGFP) vector to produce fusion proteins with EGFP (Beyotime Biotechnology, China). For *in vitro* transcription assays, full-length and truncated fragments of *IncMGPF* and *AK394747* were cloned into the pGEM-3Z vector (Promega, USA). Full-length sequences of *IncMGPF*, *MyoD*, *MEF2C*, *HuR*, and *AK394747* were amplified using specific F/R primers (Supporting Information, Table S3); the primers used to amplify the truncated fragments of

*IncMGPF* and *AK394747* are listed in Supporting Information, Table S5. For cell transfection, we transfected C2C12 myoblasts, HeLa cells, PK cells, and mouse myogenic progenitor cells with approximately 4  $\mu$ g plasmid using 9  $\mu$ L Lipofectamine 2000 (Invitrogen, USA) in each well of a 6-well plate.

### Lentivirus packaging and infection

To construct lentivirus-mediated overexpression vectors for *IncMGPF*, *AK394747*, and *hIncMGPF*, sequences of *IncMGPF*, *AK394747* and *hIncMGPF* were separately subcloned into the lentivirus vector PCDH-CMV-copGFP (Addgene, USA). To construct the lentivirus-mediated interference vector for *AK394747*, siRNA targeting *AK394747* was inserted into the SuperSilencing short hairpin RNA expression vector pLKO.1-TRC (Addgene, USA). We packaged the lentivirus in 293T cells using three vectors: 10.7  $\mu$ g pLKO.1-TRC or PCDH-CMV-copGFP, 8.0  $\mu$ g psPAX2 (Addgene, USA), and 5.3  $\mu$ g PDM2.G (Addgene, USA). For lentivirus infection of cells, 10  $\mu$ L virus and 1  $\mu$ g polybrene were added to each millilitre of medium and then replaced with fresh medium after 24 h. For mouse muscle infection, we injected 50  $\mu$ L *IncMGPF*, *AK394747*, or *hIncMGPF* overexpression lentivirus vector and empty lentivirus vector into the Gas muscles of the left and right legs, respectively, of five 1-month-old *IncMGPF* knockout (KO) mice or wild-type (WT) mice every 7 days. For pig muscle infection, we injected 1 mL *AK394747* overexpression lentivirus vector and empty lentivirus vector into the *biceps femoris* muscles of the left and right legs, respectively, of three 1-month-old pigs every 7 days. Gas and *biceps femoris* muscles were sampled after 4 weeks of weekly injections. The lentivirus concentration used in all the assays was above  $1 \times 10^8$  transducing units per millilitre. The multiplicity of infection was 10, 15, and 25 plaque forming unit per cell for the infections of C2C12 myoblasts, pig myogenic progenitor cells, and human skeletal muscle myoblasts, respectively. All primers used for plasmid construction and lentivirus production are presented in Table S3. The *hIncMGPF* sequence was synthesized by Beijing TSINGKE Biotechnology Corporation and constructed into the lentivirus vector PCDH-CMV-copGFP (Addgene, USA).

### Chromatin immunoprecipitation assay

Chromatin immunoprecipitation (ChIP) was performed using a ChIP Kit (Millipore, USA) according to the manufacturer's protocol. We performed each ChIP assay using 1  $\mu$ g antibodies. The antibodies included MyoD (sc-760; Santa Cruz Biotechnology, USA). Immunoglobulin G was used as the negative control. We conducted qRT-PCR using the retrieved DNA and primers to determine the enrichment levels of

MyoD at certain DNA loci. The primers used for ChIP-qRT-PCR are presented in *Table S1*.

### Cell proliferation assays

Cell proliferation was determined through 5-ethynyl-2'-deoxyuridine (EdU) staining, real-time cell proliferation monitoring, and Cell Counting Kit-8 (CCK-8) assays. EdU staining was conducted using the BeyoClick™ EdU Cell Proliferation Kit (Beyotime Biotechnology, China) according to the manufacturer's instructions. The cells cultured in DMEM supplemented with 50 μM EdU and 20% FBS for 2 h, at 37°C and 5% CO<sub>2</sub>. Real-time cell proliferation monitoring was performed using the xCELLigence real-time cell analyses (RTCA) system as described previously.<sup>33</sup> CCK-8 assay was conducted using the CCK-8 (BOSTER, China) according to the manufacturer's instructions.

### Western blotting

Proteins were extracted from muscle tissue and cells using radioimmunoprecipitation assay (RIPA) buffer with 1% (v/v) phenylmethylsulfonyl fluoride (Beyotime Biotechnology, China). Western blotting was performed according to a previously reported method.<sup>34</sup> The antibodies used included MyoG (sc-12732; 1:200; Santa Cruz Biotechnology, USA), MyoD (sc-760; 1:200; Santa Cruz Biotechnology, USA), MyHC (sc-376157; 1:1000; Santa Cruz Biotechnology, USA), β-actin (sc-4777; 1:1000; Santa Cruz Biotechnology, USA), MEF2C (sc-365862; 1:200; Santa Cruz Biotechnology, USA), N-Ras (sc-31; 1:200; Santa Cruz Biotechnology, USA), Ki67 (ab16667; 1:1000; Abcam, UK), HuR (sc-5261; 1:200; Santa Cruz Biotechnology, USA), Histone H3 (17168-1-AP; 1:1000; Proteintech, USA), α-tubulin (1E4C11; 1:1000; Proteintech, USA), GFP (50430-2-AP; 1:1000; Proteintech, USA), and GAPDH (sc-47724; 1:1000; Santa Cruz Biotechnology, USA). All protein levels were normalized to that of the housekeeping protein β-actin, and densitometric quantification of the western blotting bands was performed using ImageJ software.

### Cell immunofluorescence staining

Cell immunofluorescence staining was performed according to a previously published method.<sup>19</sup> Immunofluorescence staining antibodies included MyHC (sc-376157; 1:200; Santa Cruz Biotechnology, USA), MyoG (sc-12732; 1:200; Santa Cruz Biotechnology, USA), HuR (sc-5261; 1:200; Santa Cruz Biotechnology, USA), myosin (M4276; 1:1000; Sigma, USA), and a secondary antibody (anti-mouse CY3; Beyotime Biotechnology, USA). DAPI was used to visualize cell nuclei with a fluorescence microscope (DP80; Olympus, Japan). The differentiation index was calculated as the percentage of

nuclei in MyHC positive cells, and the fusion index was calculated as the percentage of nuclei in fused myotubes which have two or more nuclei out of the total nuclei.<sup>35</sup>

### Generation of IncMGPF knockout mice and measurement of phenotypes

We generated *IncMGPF* KO mice using the CRISPR genome-editing system with the C57BL/6 background according to a previous report.<sup>36</sup> Two single-guide RNAs (sgRNAs) (sgRNA1: 5'-CCTGTTGGATAATGGGGTCATGT-3'; sgRNA2: 5'-CTTAGCTTCTAGTTCGAATTCGG-3') were designed using an online CRISPR design tool (<http://tools.genome-engineering.org>) to delete the 1896 bp genomic region containing the complete *IncMGPF* transcript, and these sgRNAs were inserted into the px459 vector (Addgene, USA). The purified sgRNA-Cas9-px459 vector was injected into fertilized eggs, and successful KO was validated through PCR amplification with the specific primers (F: 5'-AGTGTCTAAATAGAGCCATGAGATGA-3'; R: 5'-GGTGTGCTTAGATAACGCTCAGGT-3'). WT mice had an amplicon size of 2262 bp, whereas KO mice possessed an amplicon of only 366 bp. The founder mice were randomly mated to produce offspring for further experiments. Male and female KO and WT offspring mice were randomly selected and their body weights measured weekly. The whole leg, Gas, transverse abdominal (TA), and Qu muscles of KO and WT mice were collected and weighed at 2 months of age. A strength test was performed according to a previously published method.<sup>37</sup> In this test, we measured the maximum muscle force three times using a grip strength meter (BIO-GS3; Bioseb, France). Exercise endurance was measured with a forced swimming test, as previously reported.<sup>37</sup> Briefly, healthy adult mice were placed into water simultaneously. A stopwatch was used to determine the time until each mouse sank into the water. The water was maintained at a constant temperature, usually of 25°C–30°C. The tester was blinded to the experimental conditions.

### Muscle injury and regeneration

Muscle injury was performed as reported previously.<sup>38</sup> Briefly, we injected 50 μL, 10 mM cardiotoxin (CTX) (Sigma, USA) in phosphate-buffered saline into the TA muscles of 8-week-old male mice and injected 100 μg EdU (Thermo Fisher Scientific, USA) intraperitoneally 4 h before harvesting muscles.

### Histology staining

Haematoxylin and eosin staining of muscle sections was performed according to a previously reported method<sup>23</sup> and

visualized using an optical microscope (BX53; Olympus, Japan). The cross-sectional areas of individual myofibres were quantified using ImageJ software. Immunohistochemical staining was performed as described previously<sup>39</sup> and visualized using a confocal laser scanning microscope (LSM800; Zeiss, Germany). For immunofluorescence staining, samples were repaired in 0.01 M sodium citrate solution (pH 6.0) for 30 min at 70°C, and incubated in blocking buffer (5% goat serum, 2% bovine serum albumin, 0.1% Triton X-100 and 0.1% sodium azide in phosphate-buffered saline) for 2 h. Samples were then incubated with primary antibodies diluted in blocking buffer overnight at 4°C. After washing with phosphate-buffered saline, the samples were incubated with secondary antibodies for 1 h at 37°C. And lastly, the samples were incubated with DAPI for 10 min at room temperature. The antibodies used included dystrophin (ab-15277; 1:100; Abcam, UK), embryonic MyHC (eMyHC) (BF-G6; 1:100; Developmental Studies Hybridoma Bank, USA), MyoG (sc-12732; 1:200; Santa Cruz Biotechnology, USA), Pax7 (1:100; Developmental Studies Hybridoma Bank, USA), COX4 (1:1000, ABclonal, A6564) and a secondary antibody (anti-mouse CY3 and anti-rabbit FITC; Beyotime Biotechnology, USA). To detect EdU incorporation, we incubated the slides using the Life Technologies Click-iT Kit (Invitrogen, USA) according to the manufacturer's instructions. Myosin ATPase staining of muscle sections was performed according to a previously reported method.<sup>39</sup> Briefly, a frozen muscle section was incubated for 2 min in pre-hybridization buffer containing 50 mM potassium acetate and 70 mM CaCl<sub>2</sub> (pH 10.4). Then, the frozen muscle section was washed three times in 100 mM Tris/HCl buffer containing 20 mM CaCl<sub>2</sub> (pH 7.2). Finally, the frozen section was incubated for 25 min in hybridization buffer containing 2.5 mM ATP disodium salt, 40 mM glycine, and 18 mM CaCl<sub>2</sub> (pH 9.4).

### Bioinformatics analyses

We predicted protein-coding capability using coding potential calculator (CPC) (<http://cpc.cbi.pku.edu.cn/>) and predicted putative transcription factor binding sites in DNA sequences using PROMO ([http://algggen.lsi.upc.es/cgi-bin/promo\\_v3/promo/promoinit.cgi?dirDB=TF\\_8.3](http://algggen.lsi.upc.es/cgi-bin/promo_v3/promo/promoinit.cgi?dirDB=TF_8.3)). We predicted the targeted miRNAs corresponding to *IncMGPF* using RNAhybrid 2.12 (<http://bibiserv.techfak.uni-bielefeld.de/rnahybrid/>) and RegRNA 2.0 (<http://regrna2.mbc.nctu.edu.tw/>). Finally, we predicted HuR binding sites using the online program Starbase 2.0 (<http://starbase.sysu.edu.cn/index.php>).

### RNA immunoprecipitation assay

RNA immunoprecipitation (RIP) was performed using the Magna RIP RNA-Binding Protein Immunoprecipitation Kit

(Millipore, USA) according to the manufacturer's instructions. The Ago2 antibody (ab3748; Abcam, UK) and HuR (sc-5261; 1:200; Santa Cruz Biotechnology, USA) were used for RIP. Co-precipitated RNA was detected using reverse transcription PCR (RT-PCR) or qRT-PCR. The qRT-PCR data are presented as a percentage of the input, as described previously.<sup>40</sup>

### Biotin-labelled RNA pulldown and mass spectrometry

Biotin-labelled RNA pulldown was performed according to a previously published method.<sup>20</sup> For mass spectrometry, the proteins pulled down with *IncMGPF* were separated using a 10% sodium dodecyl sulfate polyacrylamide gel electrophoresis (SDS-PAGE) gel and then subjected them to the silver staining. The differentially expressed bands were cut out and analysed using mass spectrometry (Novogene, China). The procedures for the *IncMGPF* and miR-135a-5p binding assay were the same as those for RNA pulldown, except that the captured RNA was purified and analysed via qRT-PCR.

### RNA stability analyses

RNA stability analyses were performed as described previously.<sup>32</sup> Briefly, C2C12 cells, mouse primary myoblasts, and pig primary myoblasts were induced to differentiate for 3 days. Then, the differentiated cells were treated with actinomycin D (ActD) (5 µg/mL), and samples were collected at 0, 1, 2, 3, and 4 h after ActD treatment. Total RNAs were extracted using Trizol (Invitrogen, USA), and reverse-transcribed using RevertAid Reverse Transcriptase (Thermo Scientific, USA). The relative RNA expression at different time points was determined using qRT-PCR.

### Statistical analyses

We calculated correlations between the expression of various lncRNAs and the *MyoD* gene using the Pearson correlation method based on previously reported microarray data (accession number: GSE102098). All differences between groups were analysed using unpaired or paired Student's *t*-test.  $P < 0.05$  was considered statistically significant; significance is denoted as \* $P < 0.05$  and \*\* $P < 0.01$ . All data are presented as mean ± standard deviation.

### Accession numbers

The microarray data generated in this study have been deposited in the Gene Expression Omnibus database (accession number: GSE138022).

## Results

### *IncMGPF is a muscle-enriched long non-coding RNA that is positively regulated by MyoD during myogenesis*

To screen for potential functional lncRNAs related to MRF-mediated regulatory network for myogenesis, we analysed the correlations between the expression of lncRNAs and the myogenic regulatory gene *MyoD* during C2C12 myoblast differentiation based on our previously reported microarray data (accession number: GSE102098). We found that the expression of 19 uncharacterized lncRNAs was highly correlated with that of the *MyoD* gene ( $|r| \geq 0.9$ ,  $P < 0.05$ ; Supporting Information, Table S4). From among these lncRNAs, we selected AK003290 (*IncMGPF*), which had the highest expression during cell differentiation, for further investigation (Figure 1A). RACE and northern blot assays confirmed that *IncMGPF* is a 1795 nt polyadenylated lncRNA (Supporting Information, Figure S1A and S1B). Protein-coding potential prediction using CPC and an *in vitro* translation experiment of the predicted open reading frame indicated that *IncMGPF* is a non-coding RNA similar to the known lncRNAs *HOTAIR* and *NEAT1* (Figure S1C and S1D). Results of qRT-PCR showed that *IncMGPF* was highly expressed in muscle tissues such as the *longissimus dorsi*, leg muscle, tongue, and heart when  $\beta$ -actin and *GAPDH* were used as reference genes, respectively (Figures 1B and S1E). Furthermore, *IncMGPF* expression increased during C2C12 myoblast differentiation as well as during embryonic and postnatal muscle development (Figures 1C and 1D and S1F and S1G). Cell fractionation assays and RNA FISH demonstrated that *IncMGPF* is mainly localized to the nucleus of proliferating myoblasts, whereas it accumulates in the cytoplasm during myogenic differentiation (Figure 1E and 1F).

To explore the mechanisms through which *IncMGPF* is regulated at the transcriptional level, we conducted luciferase assays with four reporter constructs containing different fragments of the *IncMGPF* promoter (located between -2000 and +200 bp). The region between -345 and +200 bp had the highest transcriptional activity, which suggests that this region is the core promoter (Figure S1H). Two potential MyoD binding sites (E-box) in the core promoter of *IncMGPF* were predicted through bioinformatics analyses (Figure 1H). Overexpression of *MyoD* increased the luciferase activity of reporter constructs containing predicted MyoD binding sites (-345 ~ +200 bp) and full-length reporter constructs (-2000 ~ +200 bp) (Figure S1I). *MyoD* knockdown and overexpression decreased significantly and increased the expression of endogenous *IncMGPF*, respectively (Figures 1G and S1J). Moreover, results of a ChIP assay confirmed that MyoD could physically bind to the E-box between +65 and +69 bp downstream the transcription start site of *IncMGPF*

(Figure 1H). Collectively, these data reveal that *IncMGPF* is positively regulated by the *MyoD* gene.

### *IncMGPF promotes myogenic differentiation in C2C12 myoblasts*

To explore the possible role of *IncMGPF* in myogenesis, we used microarrays to analyse changes in gene expression after *IncMGPF* knockdown in C2C12 myoblasts differentiated for 2 days. We designed two siRNAs to knock down *IncMGPF* and found that cotransfection of siRNA-1 and siRNA-2 was more efficient than transfection of siRNA-1 or siRNA-2 alone (Supporting Information, Figure S2A). *IncMGPF* was successfully knocked down when  $\beta$ -actin, *GAPDH*, and *18S rRNA* were used as reference genes (Figure S2B), as shown by the results of qRT-PCR. Compared with the controls, 407 down-regulated genes (including *MYL2*, *MYH7*, *MYH8*, and *MYO7B*) and 136 up-regulated genes (including *MYF6*, *MYL1*, and *WNT7B*) were identified in *IncMGPF* knockdown cells (fold change  $\geq 1.5$ ,  $P < 0.05$ ) (Figure S2C and Supporting Information, Data Set 1). To validate the results of the microarray, we used qRT-PCR to examine changes in the expression of some differentially expressed genes after *IncMGPF* overexpression or knockdown. The results from these two techniques were generally consistent (Figure S2D–S2G). Pathway analyses indicated that the differentially expressed genes were enriched in some signalling pathways related to muscle disease and metabolism, such as cardiac muscle contraction, and hypertrophic cardiomyopathy, which suggests that *IncMGPF* might be involved in regulating muscle development (Figure S2H and S2I).

To confirm the role of *IncMGPF* in myogenesis, we used functional gain and loss assays to investigate the effects of *IncMGPF* on myoblast proliferation, differentiation, and fusion in C2C12 myoblasts. Results of RTCA using the xCELLigence assay and EdU staining for proliferating myoblast cells showed that overexpression or knockdown of *IncMGPF* had no significant effect on cell proliferation (Supporting Information, Figure S3A, S3B, S3D, and S3E). mRNA expression of the proliferation marker genes *Ki67* and *N-Ras* was likewise unchanged after overexpression and knockdown of *IncMGPF*, as demonstrated through qRT-PCR (Figure S3C and S3F). Results of qRT-PCR, western blotting, and immunofluorescence staining for differentiated C2C12 myoblasts indicated that *IncMGPF* knockdown significantly decreased mRNA and protein expression of the myogenic marker genes *MyoD*, *MyoG*, and *MyHC* (Figures 2A–2C and S4A–S4D), whereas *IncMGPF* overexpression significantly increased that of the *MyoD*, *MyoG*, and *MyHC* genes (Figures 2D–2F and S4E–S4H). Results of qRT-PCR and MyHC immunofluorescence staining for differentiated myoblasts showed that *IncMGPF* knockdown significantly decreased mRNA expression of  $\beta$ -1 integrin, a myoblast fusion marker gene (Figure S3I), and

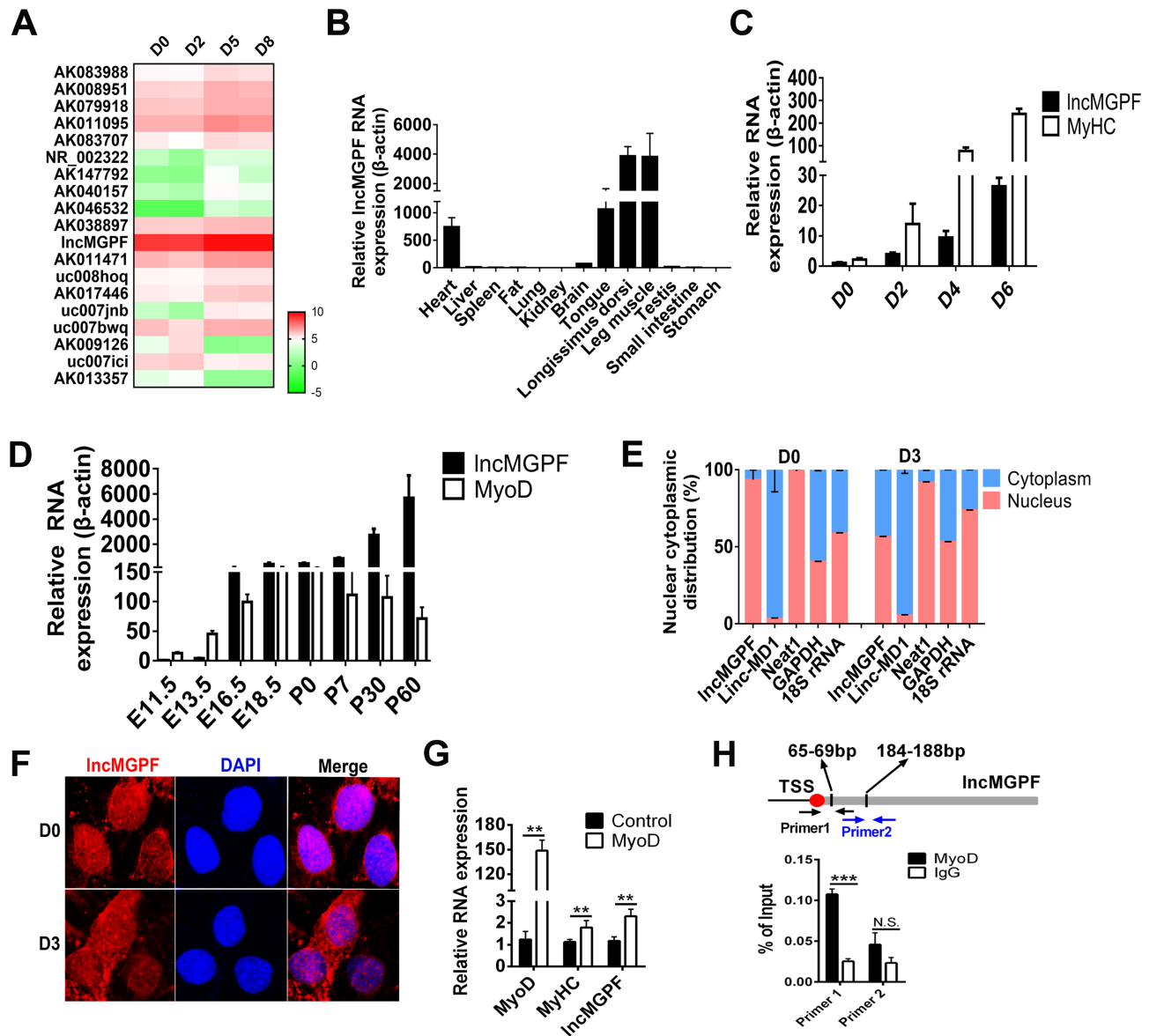


**Figure 1** Characterization and transcriptional regulation of *IncMGPF*. (A) A heatmap depicting the expression profiles of 19 uncharacterized long non-coding RNAs (lncRNAs) highly correlated with the *MyoD* gene ( $|r| \geq 0.9$ ,  $P < 0.05$ ) in proliferating (D0) C2C12 myoblasts and C2C12 myoblasts differentiated for 2 (D2), 5 (D5), and 8 days (D8). (B) Quantitative real-time PCR (qRT-PCR) shows that *IncMGPF* is highly expressed in muscle tissues including the *longissimus dorsi*, leg muscle, heart and tongue. (C, D) qRT-PCR shows that *IncMGPF* expression levels gradually increase during C2C12 myoblast differentiation (C) and from embryonic to postnatal muscle development (D). E11.5, E13.5, E16.5, and E18.5 represent embryonic days 11.5, 13.5, 16.5, and 18.5, respectively. P0, P7, P30, and P60 represent postnatal Days 0, 7, 30, and 60, respectively. *MyHC* and *MyoD* are the myogenic differentiation marker genes. (E) qRT-PCR shows the distribution of *IncMGPF* in the cytoplasm and nucleus of proliferating C2C12 myoblasts (D0) and C2C12 myoblasts differentiated for 3 days (D3). *NEAT1* and *Linc-MD1* are known nuclear and cytoplasm enriched lncRNAs, respectively, while *18S rRNA* and *GAPDH* are known to be located in both the nucleus and cytoplasm. (E) RNA FISH shows that *IncMGPF* is mainly localized to the nucleus of proliferating C2C12 myoblasts (D0) and translocates into the cytoplasm in C2C12 myoblasts differentiated for 3 days (D3). (G) qRT-PCR shows that overexpression of *MyoD* in C2C12 myoblasts differentiated for 3 days significantly increases the expression of *IncMGPF*. *MyHC* gene is a known *MyoD* target gene. (H) Chromatin immunoprecipitation-qPCR in differentiated C2C12 myoblasts shows that *MyoD* specifically binds to the E-box between 65 and 69 bp downstream the transcription start site (TSS) of *IncMGPF*. The relative RNA levels were normalized to  $\beta$ -actin. The data are presented as mean  $\pm$  standard deviation (SD) of three independent experiments; \* $P < 0.05$ , \*\* $P < 0.01$ . N.S. indicates statistical non-significance.

myoblast fusion (Figure 2C), whereas *IncMGPF* overexpression significantly increased that of the  $\beta$ -1 integrin (Figure S4J) and myoblast fusion (Figure 2F). Taken together, these

data indicated that *IncMGPF* promotes C2C12 myoblast differentiation and fusion but has no significant effects on C2C12 myoblast proliferation.



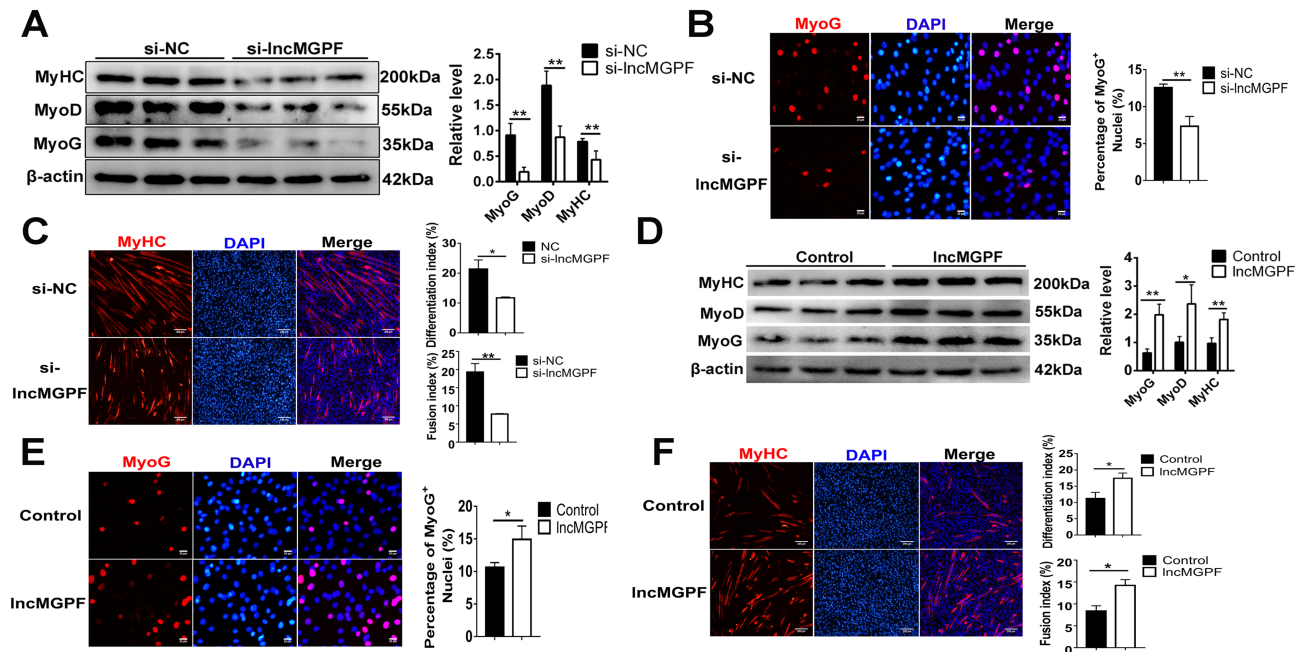


**Figure 2** *IncMGPF* promotes myogenic differentiation in C2C12 myoblasts. (A) Western blotting of differentiated C2C12 myoblasts shows that MyoD, MyoG and MyHC protein levels are significantly decreased in *IncMGPF* knockdown (*si-IncMGPF*) group compared with the negative control (*si-NC*) group. (B, C) Representative images of immunofluorescence staining for MyoG (B) and MyHC (C) in differentiated C2C12 myoblasts and quantification show that *IncMGPF* knockdown inhibits myoblast differentiation and fusion. Scale bars, 20 (B) and 200  $\mu$ m (C). (D) Western blotting of differentiated C2C12 myoblasts shows that *IncMGPF* overexpression significantly increases the MyoD, MyoG, and MyHC protein levels. (E, F) Representative images of immunofluorescence staining for MyoG (E) and MyHC (F) in differentiated C2C12 myoblasts and quantification show that *IncMGPF* overexpression promotes myoblast differentiation and fusion. Scale bars, 20 (E) and 200  $\mu$ m (F). Positively stained cells were quantified. The relative protein levels were normalized to  $\beta$ -actin. The data are presented as mean  $\pm$  SD of three independent experiments; \*  $P < 0.05$ , \*\*  $P < 0.01$ .

*IncMGPF* knockout in mice significantly decreases muscle growth and regeneration

To determine the function of *IncMGPF* in muscle development *in vivo*, we used a CRISPR/Cas9-mediated genome editing approach to inactivate *IncMGPF* in C57BL/6 mice by deleting a 1896 bp genomic region containing the complete *IncMGPF* transcript. Then we validated the genotypes using genomic DNA PCR (Supporting Information, Figure S5A). *IncMGPF* KO mice were healthy but experienced significant decreases in weight and growth rate compared with WT mice (Figures 3A, 3B, and S5B). Likewise, the weights of the whole leg, gastrocnemius (Gas), tibialis anterior (TA), and quadriceps (Qu) muscles of 2-month-old KO mice were significantly lower than those of 2-month-old WT mice in both male and female mice (Figures 3C and S5C–S5E). Haematoxylin and eosin staining and dystrophin immunofluorescence staining of muscles from 2-month-old mice showed that KO mice had significantly smaller mean cross-sectional areas of individual myofibres and higher proportions of smaller myofibres compared with WT mice (Figures 3D and S5F–S5I). DAPI staining results indicated that WT mice had ~20% more myonuclei per myofibre than KO mice (Figure 3E). In addition, there was no significant difference in the total number of satellite cells between WT and KO mice, as demonstrated by the

results of Pax7 (a specific marker of muscle satellite cells) and DAPI staining of single myofibres, as well as by Pax7 and dystrophin staining of normal muscles (Figures 3F and S5J). To confirm the effects of *IncMGPF* depletion on the expression of related genes, we examined changes in the expression of marker genes for proliferation and myogenic differentiation in the skeletal muscles of 2-month-old WT and KO mice. Compared with WT mice, KO mice showed less mRNA and protein expression of *MyoD*, *MyoG*, *MyHC*, and  $\beta$ -1 *integrin*, but no significant differences were found for the proliferation marker genes *Ki67* and *N-Ras* (Figure S5K and S5L). Although *IncMGPF* is also expressed in the heart, no significant changes in the size or weight of the heart were observed between WT and KO mice (Figure S5M). Moreover, muscle grip and forced swimming tests were used to determine muscle contractility and endurance, respectively. The results showed that both the muscle grip and endurance of KO mice were significantly lower than those of WT mice (Figure 3G and 3H). We detected cytochrome c oxidase subunit 4 (COX4; the terminal enzyme of the mitochondrial oxidative respiratory chain) in protein by immunohistochemistry and analysed the fibre type composition by myosin ATPase staining. KO mice had lower COX4 protein levels, and lower percentages of type I and oxidative fibres (Figure S5N–S5P), compared with WT mice, indicating that the reduced

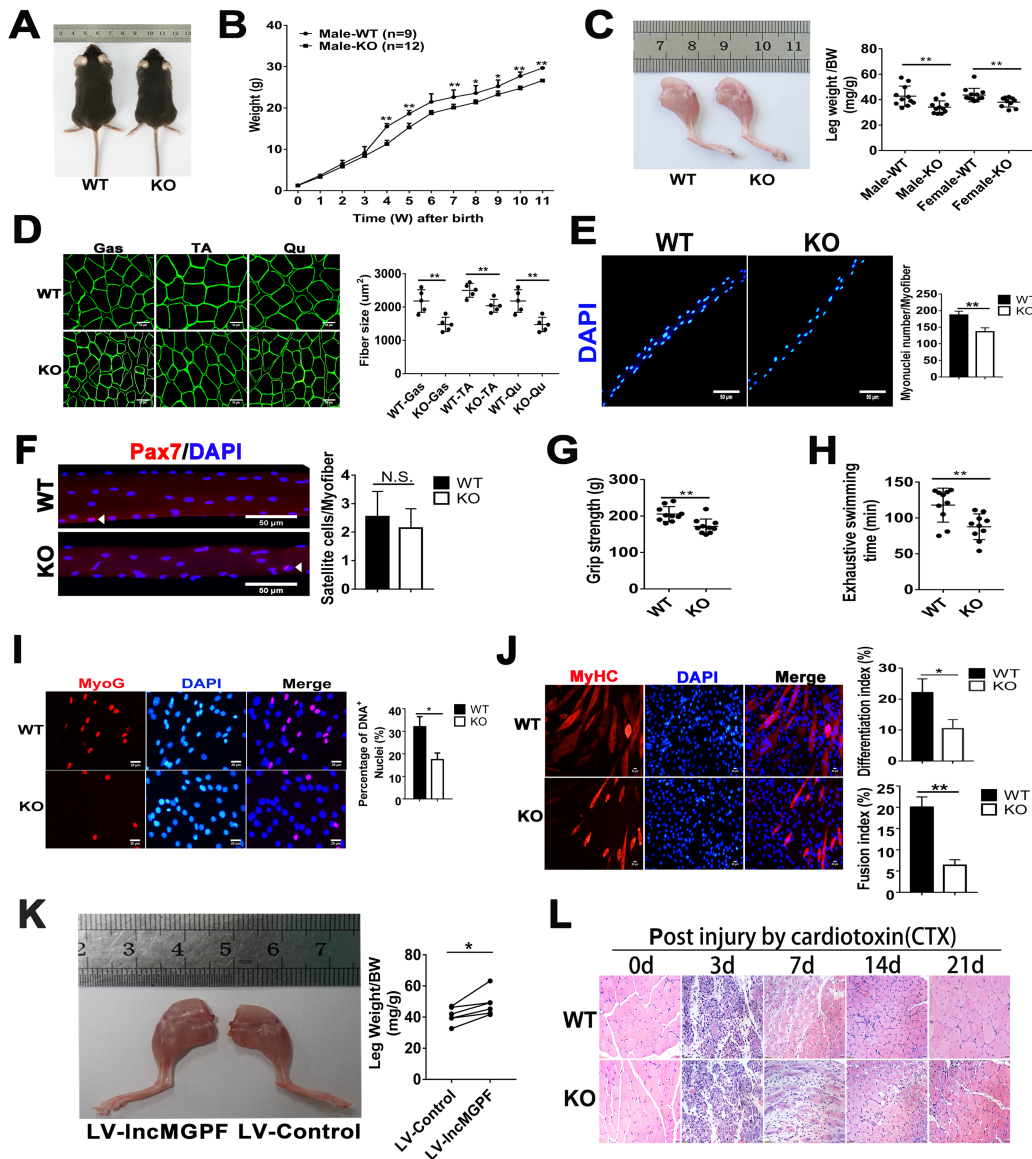


**Figure 3** *IncMGPF* knockout in mice significantly decreases muscle growth and regeneration. (A) Representative photographs of 2-month-old wild-type (WT) and knockout (KO) mice. (B) Growth curves show that WT male mice have significantly higher growth rate than KO male mice. (C) Representative photographs of the whole leg muscles of KO and WT mice and quantification show that whole leg weights of KO mice are significantly lower than those of WT mice ( $n = 11$ ). Data were normalized to the body weight (BW) (mg/g). (D) Representative images of dystrophin immunohistochemistry staining for gastrocnemius (Gas), tibialis anterior (TA), and quadriceps (Qu) muscles from 2-month-old KO and WT mice. Quantification of five independent experiments indicates that KO mice have lower average cross-sectional areas of individual myofibres than WT mice. Scale bar, 50  $\mu\text{m}$ . One hundred and fifty myofibres/muscle/mouse were analysed in an independent experiment. (E) Representative images of DAPI staining of single myofibres and quantification of five independent experiments show that *IncMGPF* knockout significantly decreases the number of myonuclei per fibre. Scale bar, 50  $\mu\text{m}$ . Twenty single myofibres/muscle/mouse were analysed in an independent experiment. (F) Representative images of Pax7 and DAPI staining of single myofibres from 2-month-old KO and WT mice. Quantification of five independent experiments indicates that there is no significant difference in the total number of satellite cells between WT and KO mice. Scale bar, 50  $\mu\text{m}$ . Twenty single myofibres/muscle/mouse were analysed in an independent experiment. The arrows indicate satellite cells. (G, H) muscle grip (G) and forced swimming (H) tests show that KO mice have less muscle contractility and endurance than WT mice ( $n = 10$ ). (I, J) Representative images of immunofluorescence staining of MyoG (I) and MyHC (J) in differentiated myogenic progenitor cells and quantification of three independent experiments show that *IncMGPF* knockout inhibits myogenic differentiation and fusion. Scale bars, 20 (I) and 50  $\mu\text{m}$  (J). (K) Representative photographs of the left and right leg muscles of KO mice injected with lentivirus-mediated *IncMGPF* overexpression (LV-*IncMGPF*) vector or control (LV-control) vector. Quantification of six independent experiments shows that overexpression of *IncMGPF* significantly increases the leg weights and rescues the muscle phenotype of KO mice;  $P$  values were determined by paired  $t$ -test. (L) Representative images of haematoxylin and eosin (H&E) staining of TA muscles at days 3, 7, 14 and 21 after injury show that *IncMGPF* promotes muscle regeneration. Scale bar, 20  $\mu\text{m}$ . The relative protein levels were normalized to  $\beta$ -actin. The data are presented as mean  $\pm$  SD of independent experiments;  $^*P < 0.05$ ,  $^{**}P < 0.01$ . Dot plot reflects data points from independent experiment.

endurance was due to a decrease in oxidative myofibres and COX4 enzyme. On the basis of these results, we concluded that *IncMGPF* promotes growth rate, muscle mass, muscle contractility, and endurance.

To further confirm the roles of *IncMGPF* in cell proliferation and differentiation in myogenic progenitor cells, we isolated primary myogenic progenitor cells from the leg muscles of WT and KO mice. Consistent with the results for C2C12 myoblasts, *IncMGPF* KO in myogenic progenitor cells had no effect on cell proliferation (Supporting Information, Figure S6A–S6D), as determined using the CCK-8, xCELLigence RTCA, EdU staining, and qRT-PCR, whereas the deletion of *IncMGPF* in myogenic progenitor cells significantly decreased myogenic progenitor cell differentiation and fusion according to results from qRT-PCR, western blotting, and immunofluorescence staining (Figures 3H and 3I and S6E and S6F). This indicates that *IncMGPF* promotes myogenic progenitor cell differentiation and fusion.

To determine whether overexpression of *IncMGPF* could rescue the muscle phenotype of KO mice, we injected the lentivirus-mediated overexpression of *IncMGPF* (LV-*IncMGPF*) vector and empty control (LV-control) vector intramuscularly into the left and right legs of 1-month-old KO mice, respectively (Supporting Information, Figure S7A). The EGFP immunofluorescence staining results showed no significant difference in infection efficiency between the LV-control and LV-*IncMGPF* groups (Figure S7B). The qRT-PCR results showed that *IncMGPF* RNA expression was significantly increased after lentivirus infection (Figure S7C). Overexpression of *IncMGPF* significantly increased the weights of the whole leg, TA, Qu, and Gas muscles, as well as the mean cross-sectional areas of individual myofibres (Figures 3J and S7D–S7G). In addition, overexpression of *IncMGPF* in KO muscles significantly increased mRNA and protein expression of *MEF2C*, *MyoD*, *MyoG*, *MyHC*, and resulted in an increased number of myonuclei per fibre (Figure S7H and S7I). These results confirmed that the decrease in muscle mass in KO mice is due to deletion of the *IncMGPF* transcript and overexpression of *IncMGPF* can rescue the muscle phenotype of KO mice. Finally, to determine the effect of *IncMGPF* overexpression in WT mice, we injected the LV-*IncMGPF* and LV-control vectors intramuscularly into the left and right legs of 1-month-old and 3-month-old growing WT mice. Consistent with the results for KO mice, there were significant increases in muscle mass, mean cross-sectional area, number of myonuclei per fibre, and myogenic gene expression after *IncMGPF* overexpression in WT muscles (Supporting Information, Figures S8 and S9). Therefore, increasing *IncMGPF* via lentivirus causes young growing muscle to grow more, but the effect of *IncMGPF* on mature muscle fibres is not known and needs to be further investigated.

To evaluate the role of *IncMGPF* in muscle regeneration, we performed a CTX-induced TA muscles injury experiment with WT and KO mice. At Day 21, muscle regeneration and

repair were almost complete in WT mice, but new formation of myofibres was ongoing in KO mice (Figure 3K). Immunofluorescence results for MyoG and eMyHC, a marker of muscle regeneration, showed that WT mice had increased numbers of MyoG positive (MyoG<sup>+</sup>) cells and eMyHC at 3 days post-injection with CTX compared with KO mice (Supporting Information, Figure S10A and S10B), which indicates that *IncMGPF* KO decreases myogenic differentiation and weakens muscle regeneration. To further test whether *IncMGPF* affects proliferation of satellite cells, we used Pax7 and EdU to compare the proliferation capacities of satellite cells in regenerating myofibres between WT and KO mice 3 days after CTX injury. As expected, no significant changes were found between WT and KO mice in the percentage of proliferating muscle satellite cells (Pax7<sup>+</sup>/EdU<sup>+</sup>) (Figure S10C). In summary, these results suggest that *IncMGPF* promotes muscle regeneration by enhancing satellite cell differentiation.

### *IncMGPF* functions as a molecular sponge of miR-135a-5p to promote myogenic differentiation

Because localization of *IncMGPF* shifts to the cytoplasm during the course of myoblast differentiation, we speculated that *IncMGPF* might function as a molecular sponge of miRNA in myogenic differentiation. To confirm the association between *IncMGPF* and the miRNA-protein complex, we performed an RIP assay for Ago2, which is the core component of the RNA-induced silencing complex. The results showed that *IncMGPF* was present in Ago2-enriched RNA (Figure 4A), which indicates that *IncMGPF* can interact with the Ago2-based miRNA-induced repression complex. Next, we identified binding sites for seven myogenesis-related miRNAs in *IncMGPF* sequences using RNAhybrid 2.12 (<http://bibiserv.techfak.uni-bielefeld.de/rnahybrid/>) and RegRNA 2.0 (<http://regRNA2.mbc.nctu.edu.tw/>) (Table S5). We cloned the full-length *IncMGPF* sequences into the region downstream of the luciferase reporter gene (Luc-*IncMGPF*) to validate the targeting of seven potential miRNAs by *IncMGPF*. The results showed that four miRNAs (miR-135a-5p, miR-221-3p, miR-133a-5p, and miR-133b-5p) could reduce luciferase activity (Figure 4B). To further screen the miRNAs associated with molecular sponge of *IncMGPF*, we examined the effects of *IncMGPF* knockdown and overexpression on expression of the target genes of the four miRNAs listed above: *MEF2C* (the target gene of miR-135a-5p), *p27* (the target gene of miR-221-3p), *IGF-1R* (the target gene of miR-133a-5p), and *MAML1* (the target gene of miR-133b-5p). *IncMGPF* knockdown and overexpression significantly decreased and increased expression of *MEF2C* (the target gene of miR-135a-5p), respectively, but no significant changes were observed in the other target genes (Figure 4C and 4D), which suggests that *IncMGPF* may regulate myogenesis via miR-135a-5p sponging. Previous studies have shown that miR-135a-5p

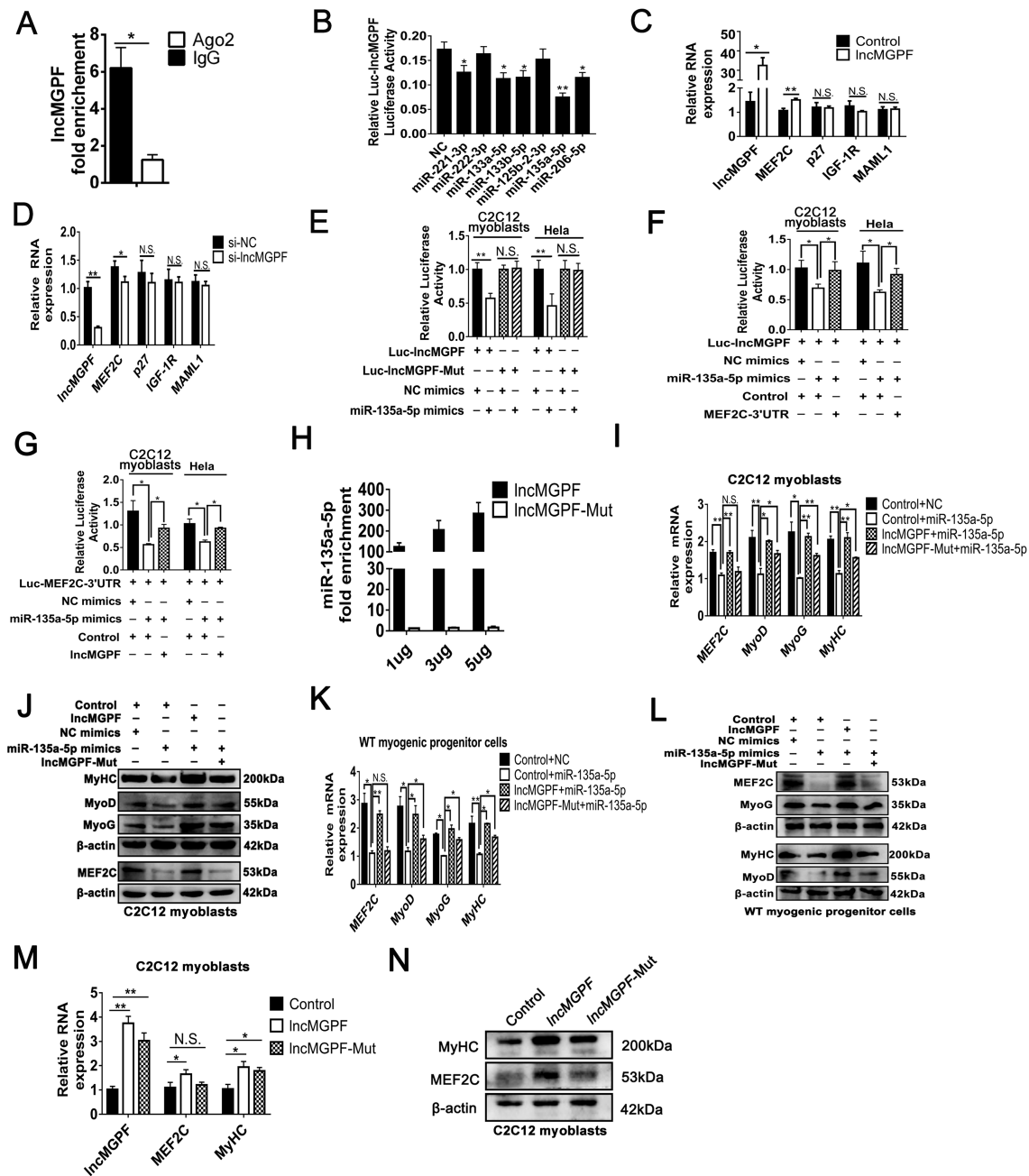


**Figure 4** *IncMGPF* functions as a molecular sponge of miR-135a-5p to promote myogenic differentiation. (A) Quantitative real-time PCR (qRT-PCR) of the RNA immunoprecipitation assay shows that *IncMGPF* can interact with Ago2 in C2C12 myoblasts differentiated for 3 days. (B) Luciferase reporter assays of *Luc-IncMGPF* in C2C12 myoblasts show that miR-135a-5p, miR-221-3p, miR-133a-5p, and miR-133b-5p reduce luciferase activities. (C, D) qRT-PCR shows that *IncMGPF* overexpression (C) and knockdown (D) in C2C12 myoblasts differentiated for 3 days significantly increase and decrease *MEF2C* mRNA expression levels, respectively, but have no significant effects on the mRNA expression of *p27*, *IGF-1R*, and *MAML1* genes. (E) Luciferase reporter assays of *Luc-IncMGPF* and *Luc-IncMGPF-Mut* in C2C12 myoblasts and HeLa cells show that miR-135a-5p specifically targets *IncMGPF*. (F, G) Luciferase reporter assays of *Luc-IncMGPF* (F) and *Luc-MEF2C-3' UTR* (G) in C2C12 myoblasts and HeLa cells show that *IncMGPF* competes with *MEF2C-3' UTR* to combine with miR-135a-5p. (H) qRT-PCR of RNA pull-down assays in C2C12 myoblasts shows that biotin-labelled *IncMGPF* specifically pulls down miR-135a-5p in a dose-dependent manner, whereas *IncMGPF-Mut* does not bind miR-135a-5p. (I–L) qRT-PCR and western blotting of C2C12 myoblasts (I, K) and myogenic progenitor cells (J, L) show that *IncMGPF* attenuates miR-135a-5p inhibition of mRNA and protein expression of *MEF2C*, *MyoD*, *MyoG*, and *MyHC* genes, and *IncMGPF-Mut* has similar activities except for the *MEF2C* gene. (M, N) qRT-PCR (M) and western blotting (N) analyses of differentiated C2C12 myoblasts show that overexpression of *IncMGPF* increases the mRNA and protein expression of *MyHC* and *MEF2C* genes, but *IncMGPF-Mut* does not affect *MEF2C* expression. The relative luciferase activity is presented as the ratio of Renilla luciferase activity to firefly luciferase activity. The relative mRNA and protein levels were normalized to  $\beta$ -actin. The miR-135a-5p RNA levels were normalized to *U6*. The data are presented as mean  $\pm$  SD of three independent experiments; \* $P < 0.05$ , \*\* $P < 0.01$ . N.S. indicates statistical non-significance.

inhibits myogenesis by targeting the *MEF2C* gene, a well-established regulator of muscle development.<sup>22,41</sup> In this study, we verified the roles of the miR-135a-5p gene in myogenic differentiation and its effect on the expression of target genes, including *lncMGPF*, *MEF2C*, *MyoD*, *MyoG*, and *MyHC*, in C2C12 myoblasts (Supporting Information, Figure S11).

To further confirm that *lncMGPF* is a target gene of miR-135a-5p, we established a WT luciferase construct of *lncMGPF* (Luc-*lncMGPF*) as well as a form in which the putative miR-135a-5p binding site was mutated (Luc-*lncMGPF*-Mut). Transfection of miR-135a-5p suppressed the luciferase activity of Luc-*lncMGPF* but had no significant effects on the luciferase activity of Luc-*lncMGPF*-Mut in C2C12 myoblasts or HeLa cells (Figure 4E). Then, we investigated whether *lncMGPF* can bind to miR-135a-5p competitively with *MEF2C*. Transfection of miR-135a-5p mimics in C2C12 myoblasts and HeLa cells led to decreased Luc-*lncMGPF* luciferase activity, whereas luciferase activity was substantially elevated after cotransfection of *MEF2C*-3' UTR (Figure 4F). Similarly, transfection of *lncMGPF* attenuated the inhibitory effects of miR-135a-5p on Luc-*MEF2C*-3' UTR luciferase activity (Figure 4G). These data demonstrate that *lncMGPF* competes with *MEF2C*-3' UTR to bind miR-135a-5p. To further confirm that *lncMGPF* interacts directly with miR-135a-5p, we incubated different amounts of biotin-labelled *lncMGPF* (1, 3, and 5 µg) with cytoplasmic lysates from C2C12 myoblasts transfected with miR-135a-5p, and we purified and analysed the RNA captured using qRT-PCR. Compared with *lncMGPF*-Mut, in which the putative miR-135a-5p binding site was mutated, biotin-labelled *lncMGPF* specifically pulled down miR-135a-5p in a dose-dependent manner (Figure 4H). Taken together, these data indicate that *lncMGPF* is a target gene of miR-135a-5p.

In addition, we performed cotransfection experiments using *lncMGPF* and miR-135a-5p overexpression vectors in C2C12 myoblasts and WT myogenic progenitor cells. Overexpression of miR-135a-5p decreased mRNA and protein expression of *MEF2C*, *MyoD*, *MyoG*, and *MyHC*, whereas cotransfection of *lncMGPF* eliminated miR-135a-5p activity. By contrast, cotransfection of *lncMGPF*-Mut did not alter the inhibitory effects of miR-135a-5p on *MEF2C* gene expression but still counterbalanced miR-135a-5p-induced inhibition of *MyoD*, *MyoG*, and *MyHC* expression (Figure 4I–L), which suggests the involvement of mechanisms other than sponging of miR-135a-5p. To further verify this possibility, we transfected the empty vector and the *lncMGPF* and *lncMGPF*-Mut vectors separately into C2C12 myoblasts. As predicted, overexpression of *lncMGPF*-Mut significantly increased expression of the *MyHC* gene but had no effect on the expression of *MEF2C*, which confirms the existence of other regulatory mechanisms (Figure 4M and 4N). Taken together, these data demonstrate that *lncMGPF* regulates

myogenesis through sponging of miR-135a-5p and other unknown mechanisms.

### *lncMGPF* interacts directly with human antigen R to promote the stabilization of *MyoD* and *MyoG* microRNAs by increasing human antigen R accumulation in the cytoplasm

As lncRNAs can regulate gene expression by interacting with multiple proteins,<sup>18,42</sup> we performed a biotin-labelled RNA pulldown assay along with SDS-PAGE staining to identify *lncMGPF*-specific binding proteins. Three specific protein bands were identified on the silver-stained SDS-PAGE gel (Supplementary Figure S12A). These specific protein bands were cut out and subjected to mass spectrometry (MS). A total of 225 binding proteins verified to contain Ago2 were identified through MS (Supporting Information, Data Set 2). From among these proteins, we selected HuR for further investigation as previous studies have shown that HuR promotes myogenic differentiation by increasing the mRNA stability of *MyoD* and *MyoG* in the cytoplasm.<sup>32,43</sup> To validate the interaction between *lncMGPF* and HuR, we performed RIP experiments in C2C12 myoblasts using the HuR antibody. The results showed that HuR interacted with *lncMGPF* in addition to known interacting RNAs for *MyoD*, *MyoG*, and *lincMD1* (Figure 5A). This interaction was validated through bio-labelled RNA pulldown (Figure 5B). Although HuR interacted with *lncMGPF*, no mutual regulation of *lncMGPF* and HuR expression was observed (Figure S12B–S12E).

As HuR enhances the mRNA stability of *MyoD* and *MyoG* by binding to AU-rich elements (AREs) in the mRNA 3' UTR,<sup>32,43</sup> we speculated that *lncMGPF* may promote myogenic differentiation by enhancing HuR-mediated mRNA stabilization of *MyoD* and *MyoG*. To validate this assumption, we transfected the overexpression vector and siRNA of *lncMGPF* into C2C12 myoblasts and then treated cells with ActD, which can inhibit the synthesis of RNA and interfere with the transcription process, to detect mRNA stability. Results of qRT-PCR showed that overexpression of *lncMGPF* increased the mRNA stability of *MyoD* and *MyoG* (Figure 5C and 5D). By contrast, knockdown of *lncMGPF* reduced the mRNA stability of *MyoD* and *MyoG* (Figure 5E and 5F). Moreover, *lncMGPF* KO in myogenic progenitor cells significantly reduced the mRNA stability of *MyoD* and *MyoG* (Supporting Information, Figure S13A and S13B). To further investigate whether *lncMGPF* enhances mRNA stability through increasing the capacity of HuR to bind to the 3' UTR of *MyoD* and *MyoG* mRNA, we performed HuR RIP assays in C2C12 myoblasts after overexpression or knockdown of *lncMGPF*. Overexpression and knockdown of *lncMGPF* significantly increased and decreased the capacity of HuR protein to bind to *MyoD* and *MyoG* mRNAs (Figure 5G and 5H), respectively. Consistent with these results, KO of *lncMGPF* in myogenic

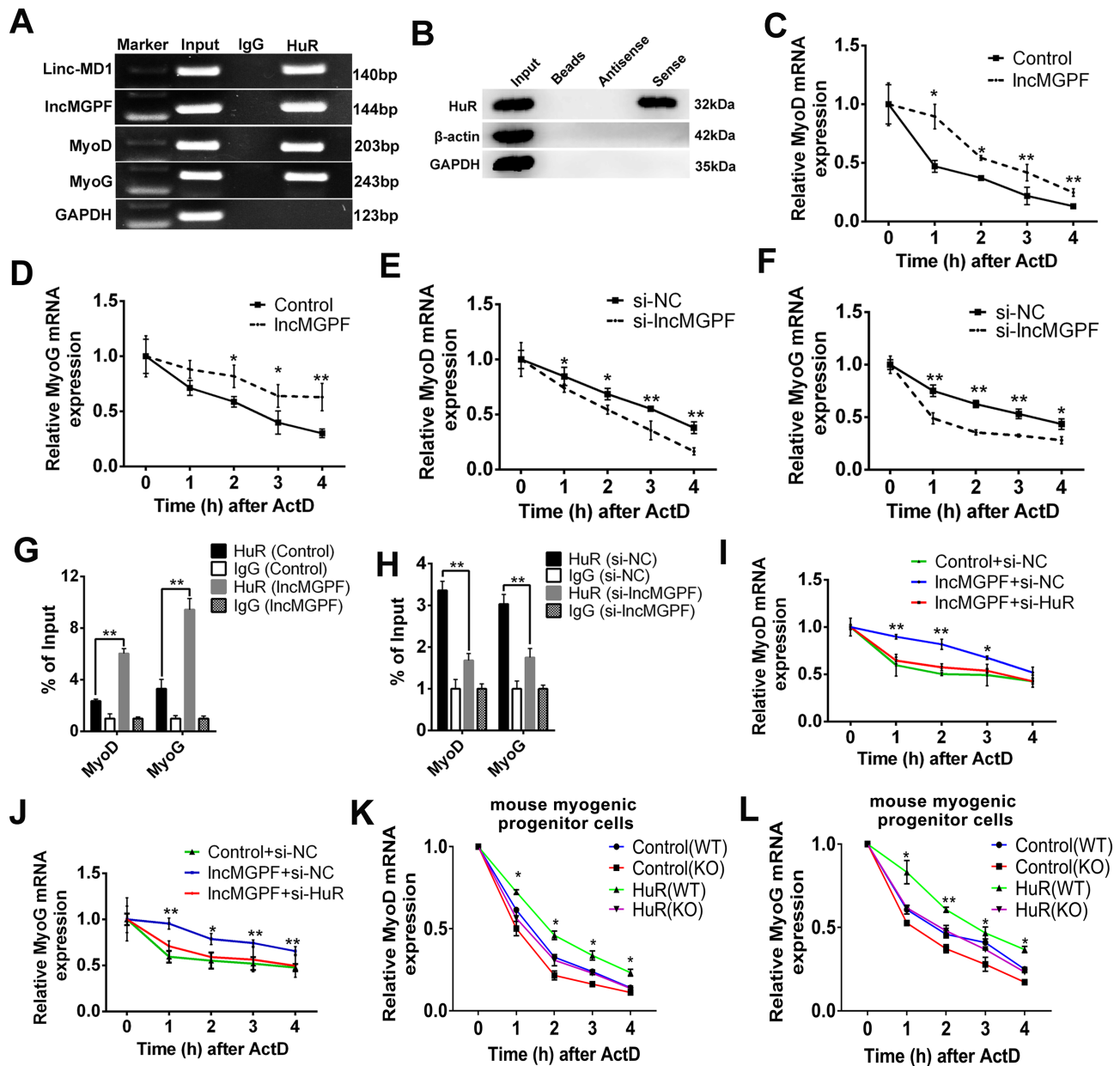


**Figure 5** *IncMGPF* directly interacts with HuR and promotes HuR-mediated mRNA stability of *MyoD* and *MyoG*. (A) RNA immunoprecipitation assays in C2C12 myoblasts show that HuR binds *IncMGPF*. Input and IgG were used as positive and negative controls, respectively. *MyoD*, *MyoG*, and *Linc-MD1* are known HuR-interacting RNAs. (B) RNA pull-down assays in C2C12 myoblasts confirm that *IncMGPF* interacts with HuR.  $\beta$ -actin and GAPDH were used as negative controls. (C–F) qRT-PCR of RNA stability assays in C2C12 myoblasts shows that *IncMGPF* overexpression significantly increases the mRNA stabilities of *MyoD* and *MyoG* genes (C, D), whereas *IncMGPF* knockdown (si-*IncMGPF*) significantly decreases *MyoD* and *MyoG* mRNA stabilities (E, F). (G, H) qRT-PCR of RIP assays in C2C12 myoblasts shows that overexpression (G) and knockdown (H) of *IncMGPF* significantly increase and decrease the binding capacities of HuR with *MyoD* and *MyoG* mRNAs, respectively. IgG was used as a negative control. (I, J) qRT-PCR of RNA stability assays in C2C12 myoblasts shows that *HuR* knockdown eliminates the promoting effects of *IncMGPF* on the mRNA stability of *MyoD* (I) and *MyoG* (J) genes. (K, L) qRT-PCR of RNA stability assays in myogenic progenitor cells shows that the mRNA stability of *MyoD* (K) and *MyoG* (L) genes are significantly increased following HuR overexpression in both WT and KO myogenic progenitor cells. The relative RNA levels were normalized to  $\beta$ -actin. The data are presented as mean  $\pm$  SD of three independent experiments; \* $P < 0.05$ , \*\* $P < 0.01$ . N.S. indicates statistical non-significance.

progenitor cells significantly decreased the ability of HuR to bind to *MyoD* and *MyoG* mRNAs (Figure S13C). Finally, we performed cotransfection experiments with the *IncMGPF* overexpression vector and HuR siRNAs in C2C12 myoblasts

to explore the effects of HuR on *IncMGPF*-mediated mRNA stabilization. The results indicated that HuR knockdown eliminated the effects of *IncMGPF* promotion of the mRNA stability of the *MyoD* and *MyoG* genes (Figure 5I and 5J). However,

the mRNA stability of the *MyoD* and *MyoG* genes increased significantly with HuR overexpression in both WT and *IncMGPF* KO myogenic progenitor cells (Figure 5K and 5L). These results suggest that *IncMGPF* regulation of target mRNA stability depends on HuR protein, but the role of HuR is not entirely dependent on *IncMGPF*.

To identify the HuR binding region of *IncMGPF*, we constructed three truncated fragments of *IncMGPF* and used them in RNA pulldown experiments. The results showed that fragment F3 (1176–1795 bp) efficiently pulled down HuR, whereas fragments F1 (1–555 bp) and F2 (556–1175 bp) rarely pulled down HuR (Figure 6A). Next, we constructed six truncated fragments of *IncMGPF* and found that fragment F7 (1630–1795 bp) was the core region involved in the interaction between *IncMGPF* and HuR (Figure 6B). Bioinformatics analyses showed that the sequence of fragment F7 contains predicted classic HuR binding motifs (GUUG, GUUUUUC) and multiple A-enriched or U-enriched sequences, which are not classic binding motifs of HuR (Figure S13D). To investigate whether the classic binding motif is necessary for *IncMGPF* to interact with HuR, we constructed the fragment lacking the classic binding motifs (F7Δ1764–1779) and performed RNA pulldown. Unexpectedly, deletion of the classic binding motifs did not affect the interaction between *IncMGPF* and HuR (Figure 6C). Next, we examined the effects of the various truncated fragments of *IncMGPF* on the mRNA stability of target genes in differentiated C2C12 myoblasts. The results showed that overexpression of full-length *IncMGPF* (FL) and truncated fragments (F7 and F7Δ1764–1779) significantly increased the stability of *MyoD* and *MyoG* mRNAs, whereas overexpression of the truncated fragment lacking the HuR binding region (F8; 1–1629 bp) did not increase the mRNA stability of the *MyoD* and *MyoG* genes (Figure 6D and 6E). To further confirm the core motif of *IncMGPF* binding to HuR, we deleted three potential binding motifs, including one classic HuR binding motif (F7Δ1764–1779) and two A/U-enriched sequences (F7Δ1730–1743; F7Δ1747–1763). The deletion of any single binding motif did not affect the binding of *IncMGPF* and HuR, while no binding of *IncMGPF* and HuR was observed after deletion of all three binding motifs (Figure 6F). These results suggested that the three motifs are independent of each other and that their binding functions are complementary. On the basis of these results, we conclude that *IncMGPF* enhances the stability of *MyoD* and *MyoG* mRNA via its HuR binding region.

Previous studies have reported that HuR protein is transferred from the nucleus to the cytoplasm during cell differentiation, and accumulation of HuR protein in the cytoplasm is required for target mRNA stabilization and pro-myogenic processes.<sup>44–46</sup> Therefore, we performed nuclear and cytoplasmic fractionation experiments to examine the effects of overexpression and knockdown of *IncMGPF* on HuR protein localization in differentiated C2C12 myoblasts. We found that

cytoplasmic HuR increased significantly with *IncMGPF* overexpression (Figure 6G and 6H), whereas knockdown of *IncMGPF* reduced HuR accumulation in the cytoplasm (Figure 6I and 6J). These observations were validated in *IncMGPF* KO and WT myogenic progenitor cells (Figure S13E and S13F). Previous studies have indicated that HuR is cleaved into two fragments, known as HuR-cleavage products 1 and 2 (HuR-CP1/2), where HuR-CP1 increases the accumulation of HuR in the cytoplasm.<sup>44,46</sup> To verify whether *IncMGPF* affects the cleavage of HuR, we determined the influence of *IncMGPF* overexpression or knockdown on protein levels of HuR-CP1 by western blotting and found that overexpression of *IncMGPF* significantly increased HuR-CP1 levels (Figure 6K), while knockdown of *IncMGPF* significantly reduced HuR-CP1 levels (Figure 6L). Taken together, these results demonstrated that *IncMGPF* enhances the stability of *MyoD* and *MyoG* mRNAs by increasing HuR cleavage and accumulation in the cytoplasm.

### *Pig long non-coding RNA AK394747 is homologous to mouse IncMGPF with conserved functions and mechanisms*

Recent studies have indicated that lncRNA exhibits cross-species conservation in terms of genomic position and RNA sequence.<sup>47,48</sup> For example, *linc-YY1* is transcribed from upstream the *YY1* promoter in the human and mouse genomes and is functionally conserved in human and mouse myogenesis.<sup>49</sup> In the UCSC Genome Browser database, we found that pig lncRNA *AK394747* has a conserved genomic position with mouse *IncMGPF* (Supporting Information, Figure S14). Both *AK394747* and *IncMGPF* are transcribed from the genomic region between the *H2AFZ* and *MTTP* genes (Figure S14A). Bioinformatics analyses showed that pig *AK394747* and mouse *IncMGPF* each have one miR-135a-5p binding site and one conserved sequence containing the HuR binding region (Figure S14B and S14C). 5' and 3' RACE assays showed that pig *AK394747* is a transcript 1586 bp in length (Supporting Information, Figure S15A). CPC analyses indicated that *AK394747* is a non-coding RNA transcript similar to the described lncRNA *HOTAIR*, *NEAT1*, and *MEG3* (Figure S15B). In addition, *AK394747* is highly expressed in skeletal muscles and is gradually up-regulated during porcine myogenic progenitor cells differentiation and postnatal muscle development (Figures 7A and 7B and S15C–S15F). Cell fractionation assays demonstrated that *AK394747* occurs mainly in the nuclei of proliferating pig myogenic progenitor cells and in the cytoplasm of differentiated cells (Figure 7C).

To determine whether *AK394747* is involved in myogenesis, we used functional gain and loss experiments to study the effects of *AK394747* on the proliferation and differentiation of pig myogenic progenitor cells. We designed

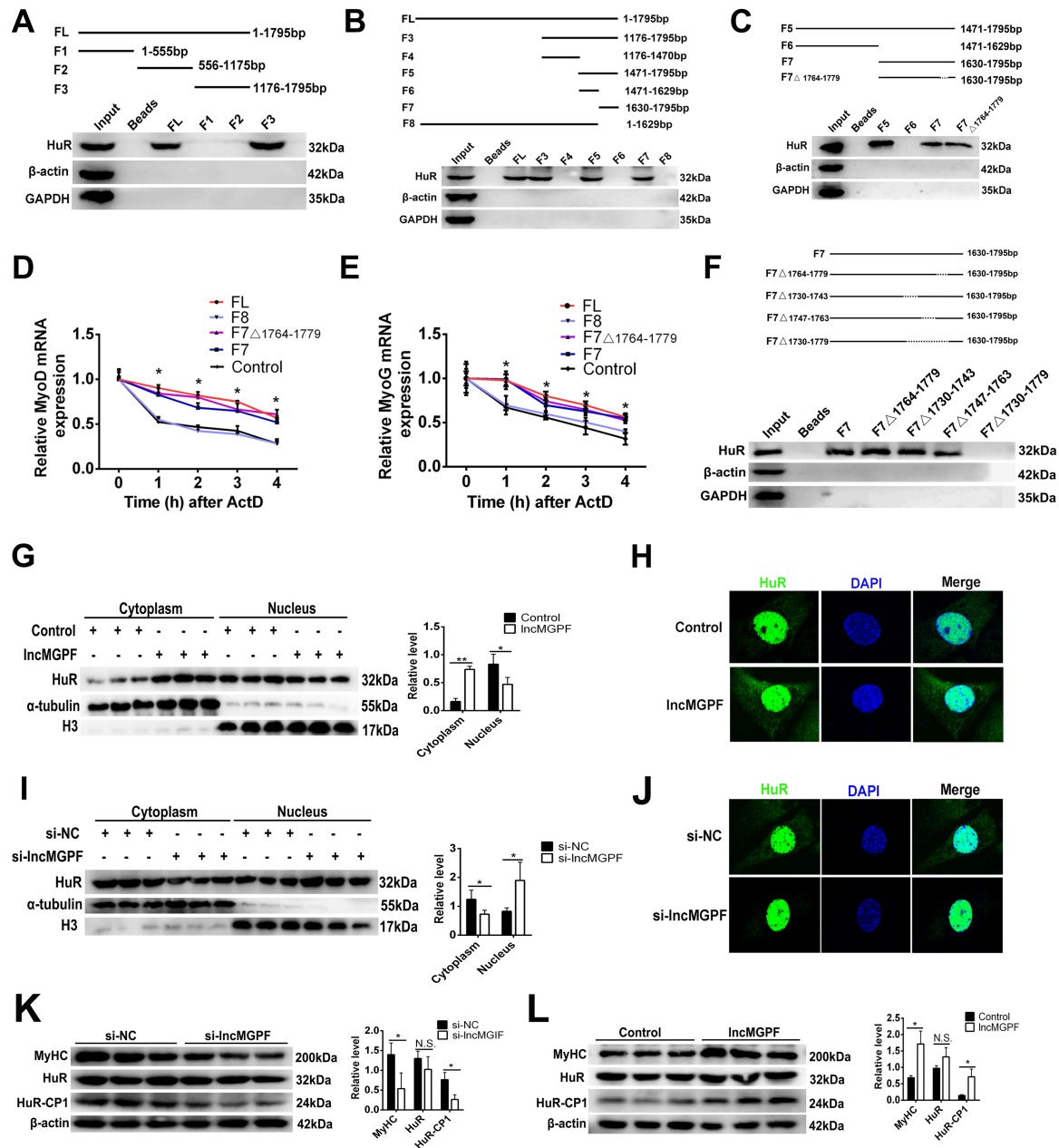


**Figure 6** *IncMGPF* regulates HuR-mediated mRNA stability through its core binding region and increases HuR accumulation in the cytoplasm. (A) RNA pull-down assays of full-length (FL) and truncated fragments of *IncMGPF* show that FL and F3 (1176–1795) specifically interact with HuR in C2C12 myoblasts.  $\beta$ -actin and GAPDH were used as negative controls. (B, C) RNA pull-down assays of truncated fragments of *IncMGPF* show that F7 (1630–1795) is the core HuR binding region for the interaction of *IncMGPF* with HuR (B) and deletion of the classical binding motifs (1764–1779) does not affect this interaction (C) in C2C12 myoblasts.  $\beta$ -actin and GAPDH were used as negative controls. (D, E) qRT-PCR of RNA stability assays in differentiated C2C12 myoblasts shows that *IncMGPF* enhances the stabilities of *MyoD* (D) and *MyoG* (E) mRNAs via the specific HuR binding region. (F) RNA pull-down assays of truncated fragments of *IncMGPF* show that the deletion of any binding motif alone (F7 $\Delta$ 1764–1779; F7 $\Delta$ 1730–1743; F7 $\Delta$ 1747–1763) does not affect the binding of *IncMGPF* and HuR, while no binding of *IncMGPF* and HuR is observed after deletion of three binding motifs simultaneously (F7 $\Delta$ 1730–1779) in C2C12 myoblasts. (G, I) Western blotting analyses of nuclear and cytoplasmic protein fractionations show that *IncMGPF* overexpression increases cytoplasmic HuR (G), whereas *IncMGPF* knockdown reduces HuR accumulation in the cytoplasm (I) in C2C12 myoblasts.  $\alpha$ -Tubulin was used as a cytoplasmic protein marker and H3 was used as a nuclear protein marker. (H, J) Representative images of HuR immunofluorescence staining assays confirm that *IncMGPF* overexpression (H) and knockdown (J) increase and decrease HuR accumulation in the cytoplasm in C2C12 myoblasts, respectively. Magnification, 63 $\times$ . (K) Western blotting of differentiated C2C12 myoblasts shows that *IncMGPF* knockdown significantly reduces and HuR-CP1 protein levels. (L) Western blotting of differentiated C2C12 myoblasts shows that *IncMGPF* overexpression significantly increases MyHC and HuR-CP1 protein levels. The relative mRNA levels were normalized to  $\beta$ -actin. The data are presented as mean  $\pm$  SD of three independent experiments; \* $P$  < 0.05, \*\* $P$  < 0.01.



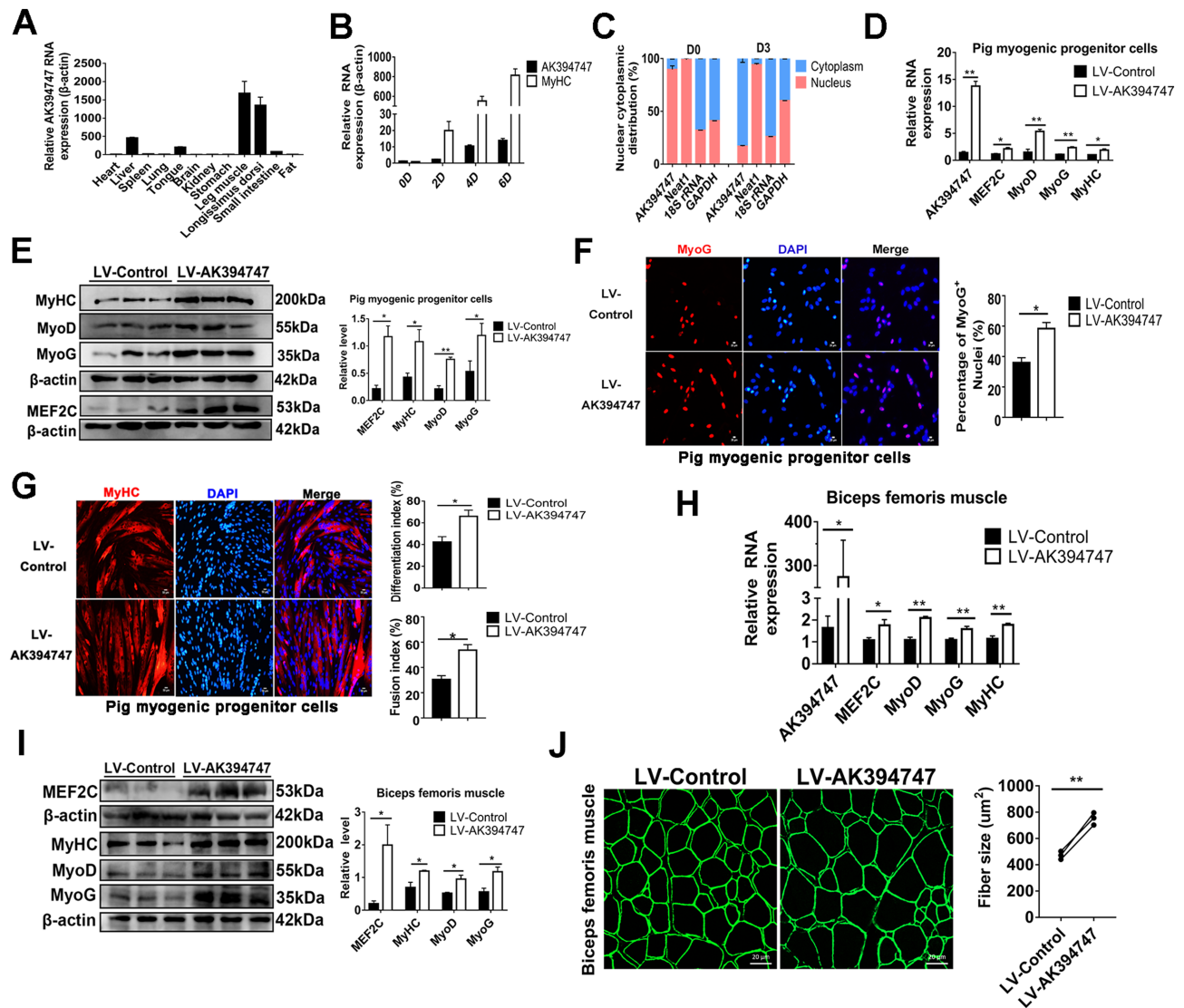


**Figure 7** Porcine *AK394747* is homologous to mouse *lncMGPF* and promotes muscle differentiation. (A) qRT-PCR shows that *AK394747* is highly expressed in muscle tissues including *longissimus dorsi* and leg muscles. (B) qRT-PCR shows that *AK394747* expression levels gradually increase during pig myogenic progenitor cell differentiation. *MyHC* is the myogenic differentiation marker gene. (C) qRT-PCR shows the distribution of *AK394747* in the cytoplasm and nucleus of proliferating pig myogenic progenitor cells (D0) and pig myogenic progenitor cells differentiated for 3 days (D3). *NEAT1* is a known nuclear lncRNA. *l8sRNA* and *GAPDH* are known to be located in both the nucleus and cytoplasm. (D, E) qRT-PCR (D) and Western blotting (E) of differentiated pig myogenic progenitor cells show that lentivirus-mediated *AK394747* overexpression (LV-*AK394747*) promotes the mRNA and protein expression of *MEF2C*, *MyoD*, *MyoG*, and *MyHC* genes. (F, G) Representative images of MyoG (F) and MyHC (G) immunofluorescence staining in differentiated pig myogenic progenitor cells and quantification show that LV-*AK394747* promotes myoblast differentiation and fusion. Scale bars, 20 (F) and 50  $\mu$ m (G). (H, I) qRT-PCR (H) and Western blotting (I) of pig *biceps femoris* muscles show that LV-*AK394747* increases the mRNA and protein expression of *MEF2C*, *MyoD*, *MyoG*, and *MyHC* genes. (J) Representative images of dystrophin immunofluorescence staining for the left and right *biceps femoris* muscles of 1-month-old piglets injected with LV-*AK394747* vector or LV-control vector. Scale bar, 20  $\mu$ m. Quantification of three independent experiments show that *AK394747* overexpression increases average cross-sectional areas of individual myofibres; *P* values were determined by paired *t*-test. One hundred and fifty myofibres/muscle/pig were analysed in an independent experiment. The relative mRNA and protein levels were normalized to  $\beta$ -actin. The data are presented as mean  $\pm$  SD of three independent experiments; \**P* < 0.05, \*\**P* < 0.01.

three siRNAs to knock down *AK394747* and found that siRNA-2 has the highest interference efficiency among three designed siRNAs in PK cells (Supporting Information, Figure S16A). Then siRNA-2 was subcloned into the lentivirus-mediated shRNA vector to infect pig myogenic

progenitor cells. Results of qRT-PCR, western blotting, and immunofluorescence staining for differentiated myogenic progenitor cells showed that lentivirus-mediated *AK394747* knockdown (LV-sh-*AK394747*) inhibited myogenic progenitor cells differentiation and fusion (Figure S16B–ES16), whereas

lentivirus-mediated overexpression of *AK394747* (LV-AK394747) promoted myogenic progenitor cells differentiation and fusion (Figure 7D–7G). However, *AK394747* did not significantly influence cell proliferation, as demonstrated by qRT-PCR, western blotting, EdU staining, and CCK-8 with proliferating myogenic progenitor cells (Supporting Information, Figure S17A–S17H). Moreover, we injected the LV-AK394747 vector and empty control (LV-control) vector into the left and right *biceps femoris* muscles of 1-month-old pigs, respectively. As expected, overexpression of *AK394747* in pigs significantly increased expression of *MEF2C*, *MyoD*, *MyoG*, and *MyHC* and the cross-sectional areas of individual myofibres (Figures 7H–7J and S17I). To further confirm that *IncMGPF* is functionally conserved between mice and pigs, we conducted the following experiments. First, we infected pig myogenic progenitor cells with LV-*IncMGPF* vector and induced differentiation for 3 days. Results from qRT-PCR, western blotting, and immunofluorescence staining showed that overexpression of mouse *IncMGPF* increased mRNA and protein expression of the myogenic marker genes *MyoD*, *MyoG*, and *MyHC* (Supporting Information, Figure S18A–S18D), which suggests that mouse *IncMGPF* promotes myogenic progenitor cells differentiation in pig. Next, we infected C2C12 myoblasts with LV-AK394747 vector and induced differentiation. As expected, overexpression of pig *AK394747* also significantly promoted C2C12 myoblast differentiation (Figure S18E–S18G). Finally, to further confirm whether pig *AK394747* could facilitate satellite cell fusion and developmental growth, we injected LV-AK394747 vector and LV-control vector intramuscularly into the left and right leg muscles of 1-month-old and 3-month-old *IncMGPF* KO mice and WT mice, respectively. The results showed that overexpression of *AK394747* significantly increased muscle weights, cross-sectional areas of individual myofibres, and myonuclei number per fibre, as well as mRNA and protein expression of the *MEF2C*, *MyoD*, *MyoG*, and *MyHC* genes (Supporting Information, Figure S19–S21). All results indicated that pig *AK394747* has functions consistent with those of mouse *IncMGPF*.

Next, we examined whether *AK394747* regulates pig myogenesis via similar mechanisms to those of mouse *IncMGPF*. An RNA pulldown assay using biotinylated *AK394747* showed that sense *AK394747* could bind with HuR, whereas the antisense RNA strand pulled down no HuR protein (Figure 8A). To determine whether the conserved sequence (1209–1556 bp) in pig *AK394747* is necessary for the interaction with HuR, we constructed four truncated *AK394747* fragments and found that fragment F3 (1380–1556 bp) corresponding to HuR binding region of mouse *IncMGPF* is required in the interaction of *AK394747* and HuR (Figure 8B). We confirmed that only overexpression of full-length *AK394747* and fragment F3 significantly increased mRNA stability of *MyoD* and *MyoG* genes in porcine myogenic progenitor cells (Figure 8C and 8D), which suggests

that *AK394747* regulates mRNA stability of these genes by interacting with HuR protein. To verify that *AK394747* regulates myogenic differentiation via miRNA sponging, we established a WT luciferase construct of *AK394747* (Luc-*AK394747*) and a form in which the putative miR-135a-5p binding site was mutated (Luc-*AK394747*-Mut) and then investigated the effects of miR-135a-5p on luciferase activity in pig myogenic progenitor cells and PK cells. The miR-135a-5p mimics significantly reduced the luciferase activity of Luc-*AK394747* but had no significant effects on that of Luc-*AK394747*-Mut (Figure 8E), which indicates that *AK394747* combined directly with miR-135a-5p as a miRNA decoy. Next, to investigate whether miR-135a-5p targets the *MEF2C* and *AK394747* genes in pig myogenic progenitor cells, we transfected miR-135a-5p mimics and an inhibitor into myogenic progenitor cells and found that overexpression and knockdown of miR-135a-5p significantly reduced and promoted, respectively, the mRNA and protein expression of target genes, including *MEF2C*, *MyoD*, *MyoG*, *MyHC*, and *AK394747* (Figure 8F and 8G and Supporting Information, Figure S22). To further demonstrate the relationship between *AK394747* and miR-135a-5p in myogenic differentiation, we performed cotransfection experiments in pig myogenic progenitor cells. Overexpression of miR-135a-5p decreased the mRNA and protein expression of *MEF2C*, *MyoD*, *MyoG*, and *MyHC* genes, whereas cotransfection of *AK394747* eliminated the effects of miR-135a-5p. When the miR-135a-5p binding site of *AK394747* was mutated (*AK394747*-Mut), cotransfection did not alter the inhibitory effects of miR-135a-5p on *MEF2C* gene expression but still counteracted miR-135a-5p inhibition of the expression of other genes (Figure 8H and 8I), consistent with the observations in mice. These results suggest that *AK394747* promotes myogenesis by up-regulating HuR-mediated mRNA stability and by acting as a miR-135a-5p sponge to enhance expression of the *MEF2C* gene.

### *IncMGPF is functionally conserved in humans*

We identified a novel transcript in human skeletal muscle myoblasts from Basic Local Alignment Search Tool analyses of the NCBI database, RT-PCR, and RACE assay verification. 5' and 3' RACE assays showed that the transcript is 1360 bp in length (Supporting Information, Figure S23A–S23C); it has been deposited in the GeneBank (accession number MT510647) and named human *IncMGPF* (*hIncMGPF*). *hIncMGPF* has a conserved genomic position with mouse and pig *IncMGPF* and contains a potential miR-135a-5p binding site and HuR protein binding motifs (Figure S23D–S23F). CPC2 analyses indicated that *hIncMGPF* is a non-coding RNA transcript similar to lncRNA *HOTAIR* and *Tsix* (Figure S23G). The *hIncMGPF* expression gradually increases with human myoblast differentiation (Figure 9A). To determine whether

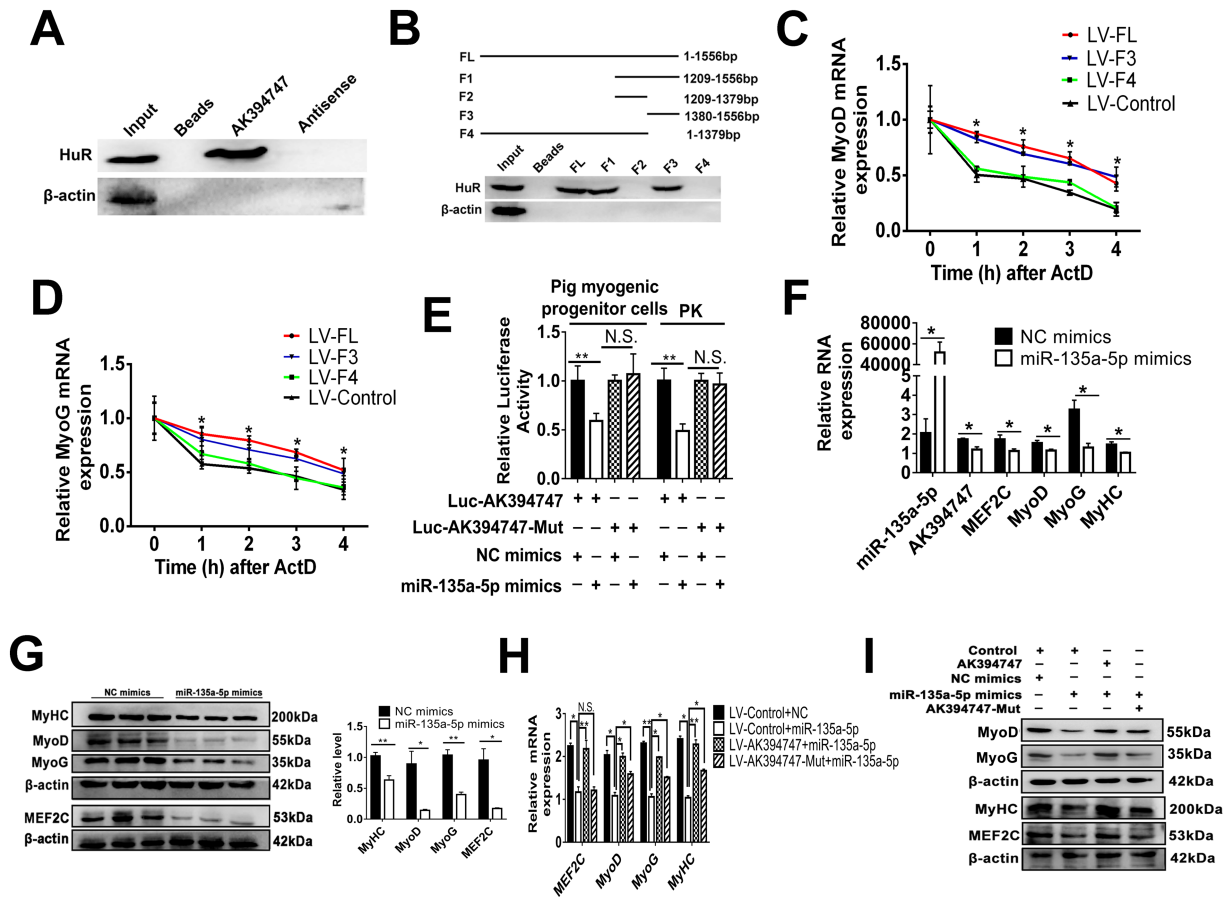


**Figure 8** *AK394747* promotes myogenesis by up-regulating HuR-mediated mRNA stability and acting as a miR-135a-5p sponge to enhance expression of the *MEF2C* gene. (A) RNA pull-down assays in pig myogenic progenitor cells show that *AK394747* interacts with HuR.  $\beta$ -actin was used as the negative control. (B) RNA pull-down assays of truncated fragments of *AK394747* in pig myogenic progenitor cells show that F3 (1380–1556) is the core binding region of *AK394747* with HuR.  $\beta$ -actin and GAPDH were used as the negative controls. (C, D) qRT-PCR of RNA stability assays in pig myogenic progenitor cells shows that *AK394747* enhances the stability of *MyoD* (C) and *MyoG* (D) mRNAs via the specific HuR binding region (F3, 1380–1556). (E) Luciferase reporter assays of *Luc-AK394747* and *Luc-AK394747-Mut* in pig myogenic progenitor cells and PK cells show that miR-135a-5p specifically targets *AK394747*. The relative luciferase activity is presented as the ratio of Renilla luciferase activity to firefly luciferase activity. (F, G) qRT-PCR (F) and Western blotting (G) of differentiated pig myogenic progenitor cells show that overexpression of miR-135a-5p reduces the mRNA or protein expression of target genes containing *MEF2C*, *MyoD*, *MyoG*, *MyHC*, and *AK394747*. (H, I) qRT-PCR (H) and Western blotting (I) show that *AK394747* attenuates miR-135a-5p inhibition of the mRNA and protein expression of *MEF2C*, *MyoD*, *MyoG*, and *MyHC* genes, and *AK394747-Mut* has similar activities with the exception of the *MEF2C* gene in pig myogenic progenitor cells. The relative RNA levels were normalized to  $\beta$ -actin. The miR-135a-5p RNA levels were normalized to *U6*. The data are presented as mean  $\pm$  SD of three independent experiments; \* $P < 0.05$ , \*\* $P < 0.01$ . N.S. indicates statistical non-significance.

*hIncMGPF* is involved in human myogenesis, we infected human skeletal muscle myoblasts with a lentivirus-mediated *hIncMGPF* overexpression (LV-*hIncMGPF*) vector and induced differentiation for 3 days. The overexpression of *hIncMGPF* significantly increased the expression of *MyoD*, *MyoG*, *MyhC*, *MEF2C*, and  $\alpha$ -actin (Figure 9B and 9C) and promoted human skeletal muscle myoblast differentiation and fusion (Figure 9D). Next, to elucidate whether *hIncMGPF* functions in skeletal muscle development, we injected the LV-*hIncMGPF* vector and LV-control vector into the left and right leg muscles of 1-month-old WT mice, respectively (Figure 9E). Consistent with the functions of *lncMGPF* in the mouse and pig, *hIncMGPF* overexpression significantly increased the muscle weights,

cross-sectional areas of individual myofibres, number of myonuclei per fibre, and expression of the *MyoD*, *MyoG*, *MEF2C*, and *MyHC* genes (Figures 9F–9L and S23H and S23I). The results indicated that *lncMGPF* is functionally conserved in humans.

## Discussion

Myogenesis is a complex process that is finely tuned by genetic and epigenetic regulatory networks. Over the past few years, researchers have identified a number of lncRNAs

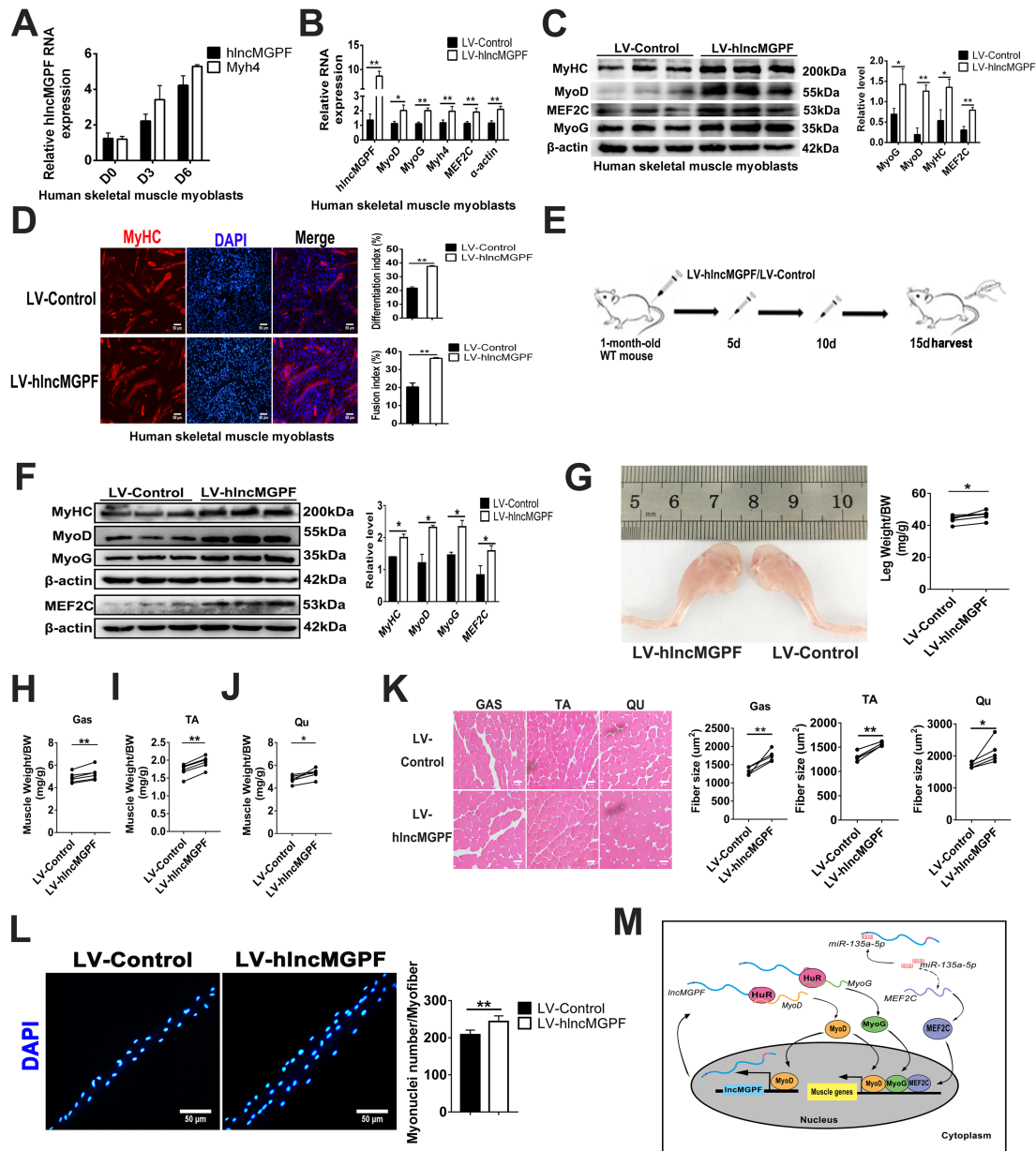


**Figure 9** *IncMGPF* is functionally conserved in humans. (A) qRT-PCR shows that the expression of *hIncMGPF* increases gradually with human myoblast differentiation.  $\beta$ -actin was used as a reference gene. *Myh4* is myogenic differentiation marker genes. (B) qRT-PCR shows that overexpression of *hIncMGPF* significantly increases the *MyoD*, *MyoG*, *Myh4*, *MEF2C*, and  $\alpha$ -actin mRNA levels in human skeletal muscle myoblasts.  $\beta$ -actin was used as a reference gene. (C) Western blotting shows that overexpression of *hIncMGPF* in human skeletal muscle myoblasts significantly increases the protein levels of MyoD, MyoG, MEF2C, and MyHC.  $\beta$ -actin was used as a reference gene. (D) Representative images of MyHC immunofluorescence staining in differentiated human skeletal muscle myoblasts and quantification show that *IncMGPF* promotes myogenic differentiation and fusion. Scale bars, 50  $\mu$ m. (E) Schematic diagram of lentivirus-mediated *hIncMGPF* overexpression (LV-*hIncMGPF*) and control (LV-control) vector injection into the Gas muscle of 1-month-old WT mice. (F) Western blotting shows that overexpression of *hIncMGPF* in the muscles of 1-month-old WT mice significantly increases MyoD, MyoG, MEF2C, and MyHC protein levels. The relative protein levels are normalized to  $\beta$ -actin. (G–J) Representative photographs of whole leg muscles injected with LV-*hIncMGPF* and LV-control vectors; the results of six independent experiments show that *hIncMGPF* overexpression significantly increases the weights of whole leg muscles (G), Gas (H), TA (I), and Qu (J) muscles; *P* values were determined by paired *t*-test. Data were normalized to body weight (BW) (mg/g). (K) Representative H&E staining images of the Gas, TA, and Qu muscles; the results of five independent experiments show that *hIncMGPF* overexpression significantly increases the average cross-sectional areas of individual myofibres. Scale bar, 50  $\mu$ m. One hundred and fifty myofibres/muscle/mouse were analysed in an independent experiment. (L) Representative images of DAPI staining of single myofibres; the results of five independent experiments show that *hIncMGPF* overexpression significantly increases the number of myonuclei per fibre. Scale bar, 50  $\mu$ m. Twenty single myofibres/muscle/mouse were analysed in an independent experiment. (M) Schematic model of *IncMGPF* regulation in myogenesis. The data in A–D, and F are the mean  $\pm$  SD of three independent experiments; \**P* < 0.05, \*\**P* < 0.01.

in skeletal muscles using high-throughput technologies such as next-generation sequencing and microarray, but few lncRNAs have been functionally annotated as key regulators of myogenesis and muscle growth. In this study, we functionally identified *lncMGPF* as a novel regulator of muscle differentiation. *lncMGPF* is highly expressed in muscles, and its expression increases gradually from embryonic to postnatal muscle development. KO of *lncMGPF* in mice substantially decreases their growth rate, reduces myofibre size and muscle mass, and impairs muscle regeneration. These data allow us to conclude that *lncMGPF* plays critical positive regulatory roles in muscle growth and regeneration. In addition, the function and mechanism of *lncMGPF* during myogenesis are conserved among mouse, pig, and human, which suggests that this lncRNA may have potential applications for treating muscle disease and improving the production of animal meat.

Recent evidence has revealed that lncRNAs may function at the post-transcriptional level.<sup>18,50</sup> In this work, we found that *lncMGPF* is transferred from the nucleus to the cytoplasm during cell differentiation and promotes myogenesis mainly through post-transcriptional regulation. On the one hand, *lncMGPF* sponges miR-135a-5p and weakens miR-135a-5p-mediated inhibition of *MEF2C* gene expression. miR-135a-5p plays critical roles in diverse biological processes and diseases, including osteoblast differentiation,<sup>51</sup> myogenic differentiation,<sup>52</sup> lung cancer,<sup>53</sup> colorectal cancer,<sup>54</sup> and prostate cancer.<sup>55</sup> Previous studies have reported that *Linc-MD1* and *MEG3* control muscle differentiation by functioning as sponges of miR-135a-5p to regulate the expression of *MEF2C*.<sup>22,56</sup> Our results add the new evidence for the notion that the miR-135a-5p/*MEF2C* axis is an important pathway in the lncRNA-mediated network of myogenesis regulation. On the other hand, *lncMGPF* modulates the mRNA stability of *MyoD* and *MyoG* genes by interacting with HuR protein. HuR is a member of the embryonic lethal abnormal vision—like family of RNA-binding proteins and is widely expressed in a variety of tissues and cells.<sup>57,58</sup> HuR increases the mRNA stability by specifically binding to AREs located in the 3' UTRs of its target transcripts.<sup>59–61</sup> lncRNAs also participate in stabilization of target mRNAs by interacting with HuR in tumorigenesis, such as *B4GALT1-AS1*,<sup>62</sup> *MIR100HG*,<sup>63</sup> *LINC00324*,<sup>64</sup> and *LINC00707*.<sup>65</sup> In muscle cells, HuR regulates myogenic differentiation and muscle fibre formation by enhancing the stability of *MyoD* and *MyoG* mRNAs.<sup>32,43,45,46,66</sup> Our data indicate that *lncMGPF* enhances the mRNA stability of myogenic genes by recruiting HuR to AREs of *MyoD* and *MyoG* genes. Bioinformatics analyses and RNA pulldown experiments identify three independent and complementary HuR binding motifs. Furthermore, we found that *lncMGPF* promotes the cleavage of HuR and increases HuR accumulation in the cytoplasm, which is necessary for HuR to function in myogenesis.<sup>44–46</sup> Therefore, we conclude that *lncMGPF*

affects the accumulation of HuR in the cytoplasm by regulating HuR cleavage.

Recent studies have revealed that lncRNAs play their roles by interacting with multiple proteins,<sup>42,67</sup> so understanding how proteins bind to particular lncRNAs is crucial to elucidating their mechanisms of action. In this study, we used RNA pulldown and MS analyses to identify 225 proteins bound to *lncMGPF*. Aside from Ago2 and HuR, we observed proteins related to m<sup>6</sup>A methylation, including writer (Mettl3) and reader (IGF2BP2, HNRNPC, and HNRNPA2B1) proteins.<sup>68–70</sup> Like mRNAs, m<sup>6</sup>A methylation of lncRNA is widespread and plays important regulatory roles in diverse biological processes; for example, the well-known lncRNA *Xist* interacts with m<sup>6</sup>A modification proteins, including writer (Mettl14, BMP15/16, WAP) and reader (YTHDC1) proteins, leading to m<sup>6</sup>A methylation of *Xist*, which is necessary for *Xist*-mediated transcriptional repression.<sup>71</sup> In addition, HuR protein is involved in m<sup>6</sup>A methylation as a reader,<sup>72</sup> and mettl3-promoted *MyoD* mRNA maintenance is required for myogenic differentiation.<sup>73</sup> Thus, it is interesting to further investigate whether the interactions of *lncMGPF* with Mettl3 and HuR are related to m<sup>6</sup>A methylation of *lncMGPF* or whether *lncMGPF* regulates *MyoD* mRNA stability through interaction and recruitment of Mettl3.

In conclusion, we have found that *lncMGPF* is a novel positive regulator of myogenesis in mice and pigs that regulates muscle differentiation at the post-transcriptional level. The *MyoD*-activated lncRNA *lncMGPF* is transferred from the nucleus to the cytoplasm during cell differentiation and promotes myogenesis mainly through post-transcriptional regulation. *lncMGPF* functions as a miRNA sponge of miR-135a-5p, weakening the inhibitory effects of miR-135a-5p on *MEF2C* and thereby increasing expression of the *MEF2C* gene. Meanwhile, *lncMGPF* increases HuR accumulation in the cytoplasm and enhances stability of *MyoD* and *MyoG* mRNAs via recruitment of HuR to AREs in the 3' UTRs of *MyoD* and *MyoG* mRNAs (Figure 9M). The *lncMGPF*/miR-135a-5p/*MEF2C* and *lncMGPF*/HuR/*MyoD*/*MyoG* pathways together constitute a novel MRF-mediated regulatory network for myogenesis.

## Funding

This work was financially supported by the National Key Project of Transgenic Research (Grant 2016ZX08006-002), the National Natural Science Foundation of China (Grant 31900448), the Agricultural Innovation Fund of Hubei Province (2016-620-000-001-043), the Fundamental Research Funds for the Central Universities (Program 2662018PY045), and the China Postdoctoral Science Foundation (Program 590319103).

## Author contributions

BZ, SZ, WL, and JJ conceived and designed the research; WL, JJ, ZX, HL, YG, XW, SW, JZ, HZ, WB, YP, and JT performed experiments; WL, JJ, ZX, and BZ analysed the data; WL, JJ, and BZ wrote the manuscript. All authors read and approved the final manuscript.

## Acknowledgements

We thank Dr Wang FC for helping in the generation of gene knockout mice. We thank Cheng YJ and Qu WP for siRNAs screening. The authors certify that they comply with the ethical guidelines for authorship and publishing of the Journal of Cachexia, Sarcopenia and Muscle.<sup>74</sup>

## References

- Godfrey R, Quinlivan R. Skeletal muscle disorders of glycogenolysis and glycolysis. *Nat Rev Neurol* 2016;**12**:393–402.
- Bowen TS, Schuler G, Adams V. Skeletal muscle wasting in cachexia and sarcopenia: molecular pathophysiology and impact of exercise training. *J Cachexia Sarcopenia Muscle* 2015;**6**:197–207.
- Wang S, Jin J, Xu Z, Zuo B. Functions and regulatory mechanisms of lncRNAs in skeletal myogenesis, muscle disease and meat production. *Cells* 2019;**8**:1107.
- Musumeci G, Castrogiovanni P, Coleman R, Szychlinska MA, Salvatorelli L, Parenti R, et al. Somitogenesis: from somite to skeletal muscle. *Acta Histochem* 2015;**117**:313–328.
- Relaix F, Zammit PS. Satellite cells are essential for skeletal muscle regeneration: the cell on the edge returns centre stage. *Development* 2012;**139**:2845–2856.
- Zammit PS. Function of the myogenic regulatory factors Myf5, MyoD, myogenin and MRF4 in skeletal muscle, satellite cells and regenerative myogenesis. *Semin Cell Dev Biol* 2017;**72**:19–32.
- Braun T, Gautel M. Transcriptional mechanisms regulating skeletal muscle differentiation, growth and homeostasis. *Nat Rev Mol Cell Biol* 2011;**12**:349–361.
- Bharathy N, Ling BM, Taneja R. Epigenetic regulation of skeletal muscle development and differentiation. *Subcell Biochem* 2013;**61**:139–150.
- Ponting CP, Oliver PL, Reik W. Evolution and functions of long noncoding RNAs. *Cell* 2009;**136**:629–641.
- Wilusz JE, Sunwoo H, Spector DL. Long noncoding RNAs: functional surprises from the RNA world. *Genes Dev* 2009;**23**:1494–1504.
- Tian D, Sun S, Lee JT. The long noncoding RNA, *Jpx*, is a molecular switch for X chromosome inactivation. *Cell* 2010;**143**:390–403.
- Martinet C, Monnier P, Louault Y, Benard M, Gabory A, Dandolo L. H19 controls reactivation of the imprinted gene network during muscle regeneration. *Development* 2016;**143**:962–971.
- Ye B, Liu B, Yang L, Zhu X, Zhang D, Wu W, et al. LncKdm2b controls self-renewal of embryonic stem cells via activating expression of transcription factor *Zbtb3*. *EMBO J* 2018;**37**:e97174.
- Kurian L, Aguirre A, Sancho-Martinez I, Benner C, Hishida T, Nguyen TB, et al. Identification of novel long noncoding RNAs underlying vertebrate cardiovascular development. *Circulation* 2015;**131**:1278–1290.
- Carpenter S, Aiello D, Atianand MK, Ricci EP, Gandhi P, Hall LL, et al. A long noncoding RNA mediates both activation and repression of immune response genes. *Science* 2013;**341**:789–792.
- Qu L, Ding J, Chen C, Wu ZJ, Liu B, Gao Y, et al. Exosome-transmitted lncARSR promotes sunitinib resistance in renal cancer by acting as a competing endogenous RNA. *Cancer Cell* 2016;**29**:653–668.
- Schmitt AM, Chang HY. Long noncoding RNAs in cancer pathways. *Cancer Cell* 2016;**29**:452–463.
- Yao RW, Wang Y, Chen LL. Cellular functions of long noncoding RNAs. *Nat Cell Biol* 2019;**21**:542–551.
- Dey BK, Pfeifer K, Dutta A. The H19 long noncoding RNA gives rise to microRNAs miR-675-3p and miR-675-5p to promote skeletal muscle differentiation and regeneration. *Genes Dev* 2014;**28**:491–501.
- Jin JJ, Lv W, Xia P, Xu ZY, Dai Zheng A, Wang XJ, et al. Long noncoding RNA SYISL regulates myogenesis by interacting with polycomb repressive complex 2. *Proc Natl Acad Sci U S A* 2018;**115**:E9802–E9811.
- Yu X, Zhang Y, Li T, Ma Z, Jia H, Chen Q, et al. Long non-coding RNA linc-RAM enhances myogenic differentiation by interacting with MyoD. *Nat Commun* 2017;**8**:14016.
- Cesana M, Cacchiarelli D, Legnini I, Santini T, Sthandier O, Chinappi M, et al. A long noncoding RNA controls muscle differentiation by functioning as a competing endogenous RNA. *Cell* 2011;**147**:358–369.
- Zhu M, Liu J, Xiao J, Yang L, Cai M, Shen H, et al. Lnc-mg is a long non-coding RNA that promotes myogenesis. *Nat Commun* 2017;**8**:14718.
- Wang J, Gong C, Maquat LE. Control of myogenesis by rodent SINE-containing lncRNAs. *Genes Dev* 2013;**27**:793–804.
- Wang L, Zhao Y, Bao X, Zhu X, Kwok YK, Sun K, et al. LncRNA Dum interacts with Dnmts to regulate Dppa2 expression during myogenic differentiation and muscle regeneration. *Cell Res* 2015;**25**:335–350.
- Gong C, Li Z, Ramanujan K, Clay I, Zhang Y, Lemire-Brachat S, et al. A long non-coding RNA, lncMyoD, regulates skeletal muscle differentiation by blocking IMP2-mediated mRNA translation. *Dev Cell* 2015;**34**:181–191.
- Zhang ZK, Li J, Guan D, Liang C, Zhuo Z, Liu J, et al. A newly identified lncRNA MAR1 acts as a miR-487b sponge to promote skeletal muscle differentiation and regeneration. *J Cachexia Sarcopenia Muscle* 2018;**9**:613–626.
- Li Z, Cai B, Abdalla BA, Zhu X, Zheng M, Han P, et al. lncIRS1 controls muscle atrophy

## Online supplementary material

Additional supporting information may be found online in the Supporting Information section at the end of the article.

**Data S1** Supporting Information

**Data S2** Supporting Information

**Data S3** Supporting Information

## Conflict of interest

The authors declare no conflict of interest.

- via sponging miR-15 family to activate IGF1-PI3K/AKT pathway. *J Cachexia Sarcopenia Muscle* 2019;**10**:391–410.
29. Yue F, Bi P, Wang C, Li J, Liu X, Kuang S. Conditional loss of Pten in myogenic progenitors leads to postnatal skeletal muscle hypertrophy but age-dependent exhaustion of satellite cells. *Cell Rep* 2016;**17**:2340–2353.
  30. Pasut A, Jones AE, Rudnicki MA. Isolation and culture of individual myofibers and their satellite cells from adult skeletal muscle. *J Vis Exp* 2013;**73**:e50074. <https://doi.org/10.3791/50074>
  31. Livak KJ, Schmittgen TD. Analysis of relative gene expression data using real-time quantitative PCR and the 2<sup>(-Delta Delta C(T))</sup> Method. *Methods* 2001;**25**:402–408.
  32. Figueroa A, Cuadrado A, Fan J, Atasoy U, Muscat GE, Munoz-Canoves P, et al. Role of HuR in skeletal myogenesis through coordinate regulation of muscle differentiation genes. *Mol Cell Biol* 2003;**23**:4991–5004.
  33. Wang S, Zuo H, Jin J, Lv W, Xu Z, Fan Y, et al. Long noncoding RNA Neat1 modulates myogenesis by recruiting Ezh2. *Cell Death Dis* 2019;**10**:505.
  34. Zhang Y, Li W, Zhu M, Li Y, Xu Z, Zuo B. FHL3 differentially regulates the expression of MyHC isoforms through interactions with MyoD and pCREB. *Cell Signal* 2016;**28**:60–73.
  35. Nie Y, Cai S, Yuan R, Ding S, Zhang X, Chen L, et al. Zfp422 promotes skeletal muscle differentiation by regulating EphA7 to induce appropriate myoblast apoptosis. *Cell Death Differ* 2020;**27**:1644–1659.
  36. Wang H, Yang H, Shivalila CS, Dawlaty MM, Cheng AW, Zhang F, et al. One-step generation of mice carrying mutations in multiple genes by CRISPR/Cas-mediated genome engineering. *Cell* 2013;**153**:910–918.
  37. Petit-Demouliere B, Chenu F, Bourin M. Forced swimming test in mice: a review of antidepressant activity. *Psychopharmacology (Berl)* 2005;**177**:245–255.
  38. Tosic M, Allen A, Willmann D, Lepper C, Kim J, Duteil D, et al. Lsd1 regulates skeletal muscle regeneration and directs the fate of satellite cells. *Nat Commun* 2018;**9**:366.
  39. Hindi SM, Shin J, Gallot YS, Straughn AR, Simionescu-Bankston A, Hindi L, et al. MyD88 promotes myoblast fusion in a cell-autonomous manner. *Nat Commun* 2017;**8**:1624.
  40. Guan H, Zhu T, Wu S, Liu S, Liu B, Wu J, et al. Long noncoding RNA LINC00673-v4 promotes aggressiveness of lung adenocarcinoma via activating WNT/beta-catenin signaling. *Proc Natl Acad Sci U S A* 2019;**116**:14019–14028.
  41. Pothoff MJ, Arnold MA, McAnally J, Richardson JA, Bassel-Duby R, Olson EN. Regulation of skeletal muscle sarcomere integrity and postnatal muscle function by Mef2c. *Mol Cell Biol* 2007;**27**:8143–8151.
  42. Chu C, Zhang QC, Da Rocha ST, Flynn RA, Bharadwaj M, Calabrese JM, et al. Systematic discovery of Xist RNA binding proteins. *Cell* 2015;**161**:404–416.
  43. van der Giessen K, Di-Marco S, Clair E, Gallouzi IE. RNAi-mediated HuR depletion leads to the inhibition of muscle cell differentiation. *J Biol Chem* 2003;**278**:47119–47128.
  44. van der Giessen K, Gallouzi IE. Involvement of transportin 2-mediated HuR import in muscle cell differentiation. *Mol Biol Cell* 2007;**18**:2619–2629.
  45. von Roretz C, Beauchamp P, Di Marco S, Gallouzi IE. HuR and myogenesis: being in the right place at the right time. *Biochim Biophys Acta* 2011;**1813**:1663–1667.
  46. Beauchamp P, Nassif C, Hillock S, Van Der Giessen K, Von Roretz C, Jasmin BJ, et al. The cleavage of HuR interferes with its transportin-2-mediated nuclear import and promotes muscle fiber formation. *Cell Death Differ* 2010;**17**:1588–1599.
  47. Ulitsky I, Shkumatava A, Jan CH, Sive H, Bartel DP. Conserved function of lincRNAs in vertebrate embryonic development despite rapid sequence evolution. *Cell* 2011;**147**:1537–1550.
  48. Washietl S, Kellis M, Garber M. Evolutionary dynamics and tissue specificity of human long noncoding RNAs in six mammals. *Genome Res* 2014;**24**:616–628.
  49. Zhou L, Sun K, Zhao YU, Zhang S, Wang X, Li Y, et al. Linc-YY1 promotes myogenic differentiation and muscle regeneration through an interaction with the transcription factor YY1. *Nat Commun* 2015;**6**:10026.
  50. Dykes IM, Emanuelli C. Transcriptional and post-transcriptional gene regulation by long non-coding RNA. *Genomics Proteomics Bioinformatics* 2017;**15**:177–186.
  51. Yin N, Zhu L, Ding L, Yuan J, Du L, Pan M, et al. MiR-135-5p promotes osteoblast differentiation by targeting HIF1AN in MC3T3-E1 cells. *Cell Mol Biol Lett* 2019;**24**:51.
  52. Li D, Deng T, Li H, Li Y. MiR-143 and miR-135 inhibitors treatment induces skeletal myogenic differentiation of human adult dental pulp stem cells. *Arch Oral Biol* 2015;**60**:1613–1617.
  53. Lin CW, Chang YL, Chang YC, Lin JC, Chen CC, Pan SH, et al. MicroRNA-135b promotes lung cancer metastasis by regulating multiple targets in the Hippo pathway and LZTS1. *Nat Commun* 2013;**4**:1877.
  54. Nagel R, le Sage C, Diosdado B, van der Waal M, Vrieling JA, Bolijn A, et al. Regulation of the adenomatous polyposis coli gene by the miR-135 family in colorectal cancer. *Cancer Res* 2008;**68**:5795–5802.
  55. Wang N, Tao L, Zhong H, Zhao S, Yu Y, Yu B, et al. miR-135b inhibits tumour metastasis in prostate cancer by targeting STAT6. *Oncol Lett* 2016;**11**:543–550.
  56. Liu M, Li B, Peng W, Ma Y, Huang Y, Lan X, et al. LncRNA-MEG3 promotes bovine myoblast differentiation by sponging miR-135. *J Cell Physiol* 2019;**234**:18361–18370.
  57. Hinman MN, Lou H. Diverse molecular functions of Hu proteins. *Cell Mol Life Sci* 2008;**65**:3168–3181.
  58. Simone LE, Keene JD. Mechanisms coordinating ELAV/Hu mRNA regulons. *Curr Opin Genet Dev* 2013;**23**:35–43.
  59. Grammatikakis I, Abdelmohsen K, Gorospe M. Posttranslational control of HuR function. *Wiley Interdiscipl Rev: RNA* 2017;**8**:e1372.
  60. Lebedeva S, Jens M, Theil K, Schwanhäusser B, Selbach M, Landthaler M, et al. Transcriptome-wide analysis of regulatory interactions of the RNA-binding protein HuR. *Mol Cell* 2011;**43**:340–352.
  61. Mukherjee N, Corcoran DL, Nusbaum JD, Reid DW, Georgiev S, Hafner M, et al. Integrative regulatory mapping indicates that the RNA-binding protein HuR couples pre-mRNA processing and mRNA stability. *Mol Cell* 2011;**43**:327–339.
  62. Li Z, Wang Y, Hu R, Xu R, Xu W. LncRNA B4GALT1-AS1 recruits HuR to promote osteosarcoma cells stemness and migration via enhancing YAP transcriptional activity. *Cell Prolif* 2018;**51**:e12504.
  63. Sun Q, Tripathi V, Yoon JH, Singh DK, Hao Q, Min KW, et al. MIR100 host gene-encoded lncRNAs regulate cell cycle by modulating the interaction between HuR and its target mRNAs. *Nucleic Acids Res* 2018;**46**:10405–10416.
  64. Zou Z, Ma T, He X, Zhou J, Ma H, Xie M, et al. Long intergenic non-coding RNA 00324 promotes gastric cancer cell proliferation via binding with HuR and stabilizing FAM83B expression. *Cell Death Dis* 2018;**9**:717.
  65. Xie M, Ma T, Xue J, Ma H, Sun M, Zhang Z, et al. The long intergenic non-protein coding RNA 707 promotes proliferation and metastasis of gastric cancer by interacting with mRNA stabilizing protein HuR. *Cancer Lett* 2019;**443**:67–79.
  66. Cammas A, Sanchez BJ, Lian XJ, Dormoy-Raclet V, Van Der Giessen K, De Silanes IL, et al. Destabilization of nucleophosmin mRNA by the HuR/KSRP complex is required for muscle fibre formation. *Nat Commun* 2014;**5**:4190.
  67. Tsai MC, Manor O, Wan Y, Mosammamaparast N, Wang JK, Lan F, et al. Long noncoding RNA as modular scaffold of histone modification complexes. *Science* 2010;**329**:689–693.
  68. Frye M, Harada BT, Behm M, He C. RNA modifications modulate gene expression during development. *Science* 2018;**361**:1346–1349.
  69. Liu J, Harada BT, He C. Regulation of gene expression by N(6)-methyladenosine in cancer. *Trends Cell Biol* 2019;**29**:487–499.
  70. Meyer KD, Jaffrey SR. Rethinking m(6)A readers, writers, and erasers. *Annu Rev Cell Dev Biol* 2017;**33**:319–342.
  71. Patil DP, Chen CK, Pickering BF, Chow A, Jackson C, Guttman M, et al. m(6)A RNA methylation promotes XIST-mediated transcriptional repression. *Nature* 2016;**537**:369–373.
  72. Shi H, Wei J, He C. Where, when, and how: context-dependent functions of RNA methylation writers, readers, and erasers. *Mol Cell* 2019;**74**:640–650.

73. Kudou K, Komatsu T, Nogami J, Maehara K, Harada A, Saeki H, et al. The requirement of Mettl3-promoted MyoD mRNA maintenance in proliferative myoblasts for skeletal muscle differentiation. *Open Biol* 2017;**7**:170119.
74. von Haehling S, Morley JE, Coats AJS, Anker SD. Ethical guidelines for publishing in the Journal of Cachexia, Sarcopenia and Muscle: update 2019. *J Cachexia Sarcopenia Muscle* 2019;**10**:1143–1145.